

**Weak precipitation,  
warm winters and  
springs impact  
glaciers of  
Mt. Everest**

F. Salerno et al.

# Weak precipitation, warm winters and springs impact glaciers of south slopes of Mt. Everest (central Himalaya) in the last two decades (1994–2013)

F. Salerno<sup>1,4</sup>, N. Guyennon<sup>2</sup>, S. Thakuri<sup>1,4</sup>, G. Viviano<sup>1</sup>, E. Romano<sup>2</sup>,  
E. Vuillermoz<sup>4</sup>, P. Cristofanelli<sup>3,4</sup>, P. Stocchi<sup>3</sup>, G. Agrillo<sup>3</sup>, Y. Ma<sup>5</sup>, and G. Tartari<sup>1,4</sup>

<sup>1</sup>National Research Council, Water Research Institute, Brugherio (IRSA-CNR), Italy

<sup>2</sup>National Research Council, Water Research Institute, Roma (IRSA-CNR), Italy

<sup>3</sup>National Research Council, Institute of Atmospheric Sciences and Climate (ISAC-CNR) Bologna, Italy

<sup>4</sup>Ev-K2-CNR Committee, Via San Bernardino, 145, Bergamo 24126, Italy

<sup>5</sup>Institute of Tibetan Plateau Research, Chinese Academy of Science, China

Received: 22 September 2014 – Accepted: 5 November 2014 – Published: 1 December 2014

Correspondence to: F. Salerno (salerno@irsa.cnr.it)

Published by Copernicus Publications on behalf of the European Geosciences Union.

Title Page

Abstract

Introduction

Conclusions

References

Tables

Figures

◀

▶

◀

▶

Back

Close

Full Screen / Esc

Printer-friendly Version

Interactive Discussion

## Abstract

Studies on recent climate trends from the Himalayan range are limited, and even completely absent at high elevation. This contribution specifically explores the southern slopes of Mt. Everest (central Himalaya), analyzing the minimum, maximum, and mean temperature and precipitation time series reconstructed from seven stations located between 2660 and 5600 m.a.s.l. over the last twenty years (1994–2013). We complete this analysis with data from all the existing ground weather stations located on both sides of the mountain range (Koshi Basin) over the same period. Overall we observe that the main and more significant increase in temperature is concentrated outside of the monsoon period. At higher elevations minimum temperature ( $0.072 \pm 0.011 \text{ }^\circ\text{C a}^{-1}$ ,  $p < 0.001$ ) increased far more than maximum temperature ( $0.009 \pm 0.012 \text{ }^\circ\text{C a}^{-1}$ ,  $p > 0.1$ ), while mean temperature increased by  $0.044 \pm 0.008 \text{ }^\circ\text{C a}^{-1}$ ,  $p < 0.05$ . Moreover, we note a substantial precipitation weakening ( $9.3 \pm 1.8 \text{ mma}^{-1}$ ,  $p < 0.01$  during the monsoon season). The annual rate of decrease at higher elevation is similar to the one at lower altitudes on the southern side of the Koshi Basin, but here the drier conditions of this remote environment make the fractional loss much more consistent (47% during the monsoon period). This study contributes to change the perspective on which climatic driver (temperature vs. precipitation) led mainly the glacier responses in the last twenty years. The main implications are the following: (1) the negative mass balances of glaciers observed in this region can be more ascribed to less accumulation due to weaker precipitation than to an increase of melting processes. (2) The melting processes have only been favored during winter and spring months and close to the glaciers terminus. (3) A decreasing of the probability of snowfall has significantly interested only the glaciers ablation zones (10%,  $p < 0.05$ ), but the magnitude of this phenomenon is decidedly lower than the observed decrease of precipitation. (4) The lesser accumulation could be the cause behind the observed lower glacier flow velocity and the current stagnation condition of tongues, which in turn could have triggered melting processes under the debris glacier coverage, leading to the formation of numerous

## Weak precipitation, warm winters and springs impact glaciers of Mt. Everest

F. Salerno et al.

Title Page

Abstract

Introduction

Conclusions

References

Tables

Figures

◀

▶

◀

▶

Back

Close

Full Screen / Esc

Printer-friendly Version

Interactive Discussion



supraglacial and proglacial lakes that have characterized the region in the last decades. Without demonstrating the causes that could have led to the climate change pattern observed at high elevation, we conclude by listing the recent literature on hypotheses that accord with our observations.

## 1 Introduction

The current uncertainties concerning the glacial shrinkage in the Himalayas are mainly attributed to a lack of measurements, both of the glaciers and of climatic forcing agents (e.g., Bolch et al., 2012). Recent results underline the need for a fine scale investigation, especially at high altitude, to better model the hydrological dynamics in this area. However, there are few high elevation weather stations in the world where the glaciers are located (Tartari et al., 2009). This can be attributed to the remote location of glaciers, the rugged terrain, and a complex political situation, all of which make physical access difficult (Bolch et al., 2012). As a consequence of the remoteness and difficulty in accessing many high elevation sites combined with the complications of operating automated weather stations (AWSs) at these altitudes, long-term measurements are challenging (Vuille, 2011). However, nearly all global climate models report increased sensitivity to warming at high elevations (e.g., Rangwala and Miller, 2012), while observations are less clear (Pepin and Lundqvist, 2008). Moreover, changes in the timing or amount of precipitation are much more ambiguous and difficult to detect, and there is no clear evidence of significant changes in total precipitation patterns in most mountain regions (Vuille, 2011).

The need for a fine scale investigation is particularly evident on the south slope of Mt. Everest (central Southern Himalaya, CH-S) as it is one of the heavily glaciated parts of the Himalaya (Salerno et al., 2012; Thakuri et al., 2014). Nevertheless, these glaciers have the potential to build up moraine-dammed lakes storing large quantities of water, which are susceptible to GLOFs (glacial lake outburst floods) (e.g., Salerno et al., 2012; Fujita et al., 2013). Gardelle et al. (2011) noted that this region is most characterized

## Weak precipitation, warm winters and springs impact glaciers of Mt. Everest

F. Salerno et al.

Title Page

Abstract

Introduction

Conclusions

References

Tables

Figures

◀

▶

◀

▶

Back

Close

Full Screen / Esc

Printer-friendly Version

Interactive Discussion



## Weak precipitation, warm winters and springs impact glaciers of Mt. Everest

F. Salerno et al.

Title Page

Abstract

Introduction

Conclusions

References

Tables

Figures

◀

▶

◀

▶

Back

Close

Full Screen / Esc

Printer-friendly Version

Interactive Discussion



by glacial lakes in the Hindu Kush Karakorum Himalaya. Recently, Thakuri et al. (2014) noted that the Mt. Everest glaciers experienced an accelerated shrinkage in the last twenty years (1992–2011), as underlined by an upward shift of the Snow Line Altitude (SLA) with a velocity almost three times greater than the previous period (1962–1992).

Furthermore Bolch et al. (2011) and Nuimura et al. (2012) found a higher mass loss rate during the last decade (2000–2010). Anyway, to date, there are not continuous meteorological time series able to clarify the causes of the melting process to which the glaciers of these slopes are subjected.

In this context, since the early 1990s, PYRAMID Observatory Laboratory (5050 m) was created by the Ev-K2-CNR Committee ([www.ev-k2-cnr.org](http://www.ev-k2-cnr.org)). This observatory is located at the highest elevation at which weather data has ever been collected in the region and thus represents a valuable dataset with which to investigate the climate change in CH-S (Tartari et al., 2002; Lami et al., 2010). However, the remoteness and the harsh conditions of the region over the years have complicated the operations of the AWSs, obstructing long-term measurements from a unique station.

In this paper, we mainly explore the small scale climate variability of the south slopes of Mt. Everest by analyzing the minimum, maximum, and mean air temperature ( $T$ ) and precipitation (Prec) time series reconstructed from seven AWSs located from 2660 to 5600 m a.s.l. over the last couple of decades (1994–2013). Moreover, we complete this analysis with all existing weather stations located on both sides of the Himalayan range (Koshi Basin) for the same period. In general, this study has the ultimate goal of linking the climate change patterns observed at high elevation with the glacier responses over the last twenty years, during which a more rapid glacier shrinkage process occurred in the region of investigation.

## 2 Region of investigation

The current study is focused on the Koshi (KO) Basin which is located in the eastern part of central Himalaya (CH) (Yao et al., 2012; Thakuri et al., 2014). To explore pos-

sible differences in the surroundings of Mt. Everest, we decided to consider the north and south parts of CH (with the suffixes -N and -S, respectively) separately (Fig. 1a). The KO River (58 100 km<sup>2</sup> of the basin) originates in the Tibetan Plateau (TP) and the Nepali highlands. The area considered in this study is within the latitudes of 27° and 28.5° N and longitudes of 85.5° and 88° E. The altitudinal gradient of this basin is the highest in the world, ranging from 77 to 8848 m a.s.l., i.e., Mt. Everest. We subdivide the KO Basin into the northern side (KO-N), belonging to the CH-N, and southern side (KO-S), belonging to the CH-S. The southern slopes of Mt. Everest are part of the Sagarmatha (Everest) National Park (SNP) (Fig. 1b), where the small scale climate variability at high elevation is investigated. The SNP is the world's highest protected area, with over 30 000 tourists in 2008 (Salerno et al., 2013). The park area (1148 km<sup>2</sup>), extending from an elevation of 2845 to 8848 m a.s.l., covers the upper Dudh Koshi (DK) Basin (Manfredi et al., 2010; Amatya et al., 2010). Land cover classification shows that almost one-third of the territory is characterized by glaciers and ice cover (Salerno et al., 2008; Tartari et al., 2008), while less than 10 % of the park area is forested (Bajracharya et al., 2010). The SNP presents a broad range of bioclimatic conditions with three main bioclimatic zones: the zone of alpine scrub; the upper alpine zone, which includes the upper limit of vegetation growth; and the Arctic zone, where no plants can grow (UNEP and WCMC, 2008). Figure 1c shows the glacier distribution along the hypsometric curve of the SNP. We observe that the glacier surfaces are distributed from 4300 to above 8000 m a.s.l., with more than 75 % of the glacier surfaces lying between 5000 and 6500 m a.s.l. The 2011 area-weighted mean elevation of the glaciers was 5720 m a.s.l. (Thakuri et al., 2014). These glaciers are identified as the summer accumulation-type fed mainly by summer Prec from the South Asian monsoon system, whereas the winter Prec caused by the mid-latitude westerly wind is minimal (Yao et al., 2012). The prevailing direction of the monsoons is S–N and SW–NE (e.g., Ichayanagi et al., 2007). The climate is influenced by the monsoon system because the area is located in the subtropical zone with nearly 90 % of the annual Prec falling in the months of June to September (this study). Heavy autumn and winter snowfalls can occur in

---

**Weak precipitation,  
warm winters and  
springs impact  
glaciers of  
Mt. Everest**F. Salerno et al.

---

[Title Page](#)[Abstract](#)[Introduction](#)[Conclusions](#)[References](#)[Tables](#)[Figures](#)[◀](#)[▶](#)[◀](#)[▶](#)[Back](#)[Close](#)[Full Screen / Esc](#)[Printer-friendly Version](#)[Interactive Discussion](#)

association with tropical cyclones and westerly disturbances, respectively, and snow accumulation can occur at high elevations at all times of the year (Benn, 2012). Bolasina et al. (2002) have demonstrated the presence of well-defined local circulatory systems in the Khumbu Valley (SNP). The local circulation is dominated by a system of mountain and valley breezes. The valley breeze blows (approximately  $4 \text{ m s}^{-1}$ ) from the south every day from sunrise to sunset throughout the monsoon season, pushing the clouds that bring Prec northward.

### 3 Data

#### 3.1 Weather stations at high elevation

The first automatic weather station (named hereafter AWS0) at 5050 m.a.s.l. near PYRAMID Observatory Laboratory (Fig. 1c), and beginning in October 1993, it has run continuously all year round (Bertolani et al., 2000). The station, operating in extreme conditions, had recorded long-term ground-based meteorological data, and the data are considered valid until December 2005. Due to the obsolescence of technology, the station was disposed of in 2006. A new station (named hereafter AWS1) was installed just a few tens of meters away from AWS0 and has been operating since October 2000. Other stations were installed in the following years in the upper DK Basin in the Khumbu Valley (Table 1). In 2008, the network included the sixth monitoring point, the highest weather station of the world, located at South Col of Mt. Everest (7986 m.a.s.l.). The locations of all stations are presented in Fig. 1b. We can observe in Fig. 1c that this meteorological network represents the climatic conditions of the SNP glaciers well: AWS0 and AWS1 (5035 m.a.s.l.) characterize the glacier fronts (4870 m.a.s.l.), AWS4 (5600 m.a.s.l.) represents the mean elevation of glaciers (5720 m.a.s.l.), and AWS5, the surface station at South Col (7986 m.a.s.l.), characterizes the highest peaks (8848 m.a.s.l.).

## Weak precipitation, warm winters and springs impact glaciers of Mt. Everest

F. Salerno et al.

Title Page

Abstract

Introduction

Conclusions

References

Tables

Figures

◀

▶

◀

▶

Back

Close

Full Screen / Esc

Printer-friendly Version

Interactive Discussion



## Weak precipitation, warm winters and springs impact glaciers of Mt. Everest

F. Salerno et al.

Title Page

Abstract

Introduction

Conclusions

References

Tables

Figures

◀

▶

◀

▶

Back

Close

Full Screen / Esc

Printer-friendly Version

Interactive Discussion



All stations, except AWS5, record at least  $T$  and Prec. This dataset presents some gaps (listed in Table 1) as a consequence of the complications of operating AWS at these altitudes. The list of measured variables for each stations and relevant data can be downloaded from <http://geonetwork.evk2cnr.org/>. Data processing and quality checks are performed according to the international standards of the WMO (World Meteorological Organization).

The Prec sensors at these locations are tipping buckets usually used for rainfall measurements and may not fully capture the solid Prec. Therefore, Prec is probably underestimated, especially in winter. In this regard, according to both Fujita and Sakai, 2014 and field observations (Ueno et al., 1994), the precipitation phase has been taken into account assuming that the probability of snowfall and rainfall depends on mean daily temperature, using – as proposed by the aforementioned authors – as thresholds 0 and 4 °C, respectively. In Fig. 2 we first of all observe that at 5050 m a.s.l. 90 % of precipitation is concentrated during June–September and that the probability of snowfall is very low (4 %), considering that the mean daily temperature during these months is above 0 °C. On a yearly basis, this probability reaches 20 % of the annual cumulated precipitation.

### 3.2 Other weather stations at lower altitude in the Koshi Basin

In KO-S Basin (Nepal), the stations are operated by the Department of Hydrology and Meteorology (DHM) ([www.dhm.gov.np/](http://www.dhm.gov.np/)). For daily  $T$  and Prec, we selected 10 stations for  $T$  and 19 stations for Prec considering both the length of the series and the monitoring continuity (< 10 % of missing daily data). The selected stations cover an elevation range between 158 and 2619 m a.s.l. (Table 3). In KO-N Basin (TP, China), the number of ground weather stations (operated by the Chinese Academy of Science, CAS), selected with the same criteria mentioned above, is considerably smaller, just two, but these stations have a higher elevation (4302 m for the Dingri station and 3811 m a.s.l. for the Nyalam station).



## 4 Methods

We define the pre-monsoon, monsoon, and post-monsoon seasons as the months from February to May, June to September, and October to January, respectively. The minT, maxT, and meanT are calculated as the minimum, maximum, and mean daily air temperature. For total precipitation (Prec), we calculate the mean of the cumulative precipitation for the analyzed period.

### 4.1 Reconstruction of the daily temperature and precipitation time series at high elevation

The two stations named AWS0 and AWS1 in the last twenty years, considering the extreme weather conditions of these slopes, present a percentage of missing daily values of approximately 20 % (Table 1). The other stations (hereafter named secondary stations) were used here for infilling the gaps according to a priority criteria based on the degree of correlation among data. AWS1 was chosen as the reference station given the length of the time series and that it is currently still operating. Therefore, our reconstruction (hereafter named PYRAMID) is referred to an elevation of 5035 m a.s.l.

The selected infilling method is a simple regression analysis based on quantile mapping (e.g., Déqué, 2007; Themeßl et al., 2012). This simple regression method has been preferred to more complex techniques, such as the fuzzy rule-based approach (Abebe et al., 2000) or the artificial neural networks (Abudu et al., 2010; Coulibaly and Evora, 2007), considering the peculiarity of this case study. In fact, all stations are located in the same valley (Khumbu Valley). This aspect confines the variance among the stations to the altitudinal gradient of the considered variable ( $T$  or Prec), which can be easily reproduced by the stochastic link created by the quantile mapping method. In case all stations registered a simultaneous gap, we apply a multiple imputation technique (Schneider, 2001) that uses some other proxy variables to fill the remaining missing data. Details on the reconstruction procedure and the computation of the associated uncertainty are provided in Supplement 1.

## Weak precipitation, warm winters and springs impact glaciers of Mt. Everest

F. Salerno et al.

Title Page

Abstract

Introduction

Conclusions

References

Tables

Figures

◀

▶

◀

▶

Back

Close

Full Screen / Esc

Printer-friendly Version

Interactive Discussion





## 4.2 The trends analysis: the Sequential Mann–Kendall test

The Mann–Kendall (MK) test (Kendall, 1975) is widely adopted to assess significant trends in hydro-meteorological time series (e.g., Carraro et al., 2012a, b; Guyennon et al., 2013). This test is non-parametric, thus being less sensitive to extreme sample values, and is independent of the hypothesis about the nature of the trend, whether linear or not. The MK test verifies the assumption of the stationarity of the investigated series by ensuring that the associated normalized Kendall's tau coefficient,  $\mu(\tau)$ , is included within the confidence interval for a given significance level (for  $\alpha = 5\%$ , the  $\mu(\tau)$  is below  $-1.96$  and above  $1.96$ ). In the sequential form (seqMK) (Gerstengarde and Werner, 1999),  $\mu(\tau)$  is calculated for each element of the sample. The procedure is applied forward starting from the oldest values (progressive) and backward starting from the most recent values (retrograde). If no trend is present, the patterns of progressive and retrograde  $\mu(\tau)$  vs. time (i.e., years) present several crossing points, while a unique crossing period allows the approximate location of the starting point of the trend (e.g., Bocchiola and Diolaiuti, 2010).

In this study, the seqMK is applied to monthly vectors. Monitoring the seasonal non-stationarity, the monthly progressive  $\mu(\tau)$  is reported with a pseudo color code, where the warm colors represent the positive slopes and cold colors the negative ones. Color codes associated with values outside of the range ( $-1.96$  to  $1.96$ ) possess darker tones to highlight the trend significance (Salerno et al., 2014). Moreover, to monitor the overall non-stationarity of the time series, both the progressive and the retrograde  $\mu(\tau)$  at the annual scale are reported. We used the Sen's slope proposed by Sen (1968) as a robust linear regression allowing the quantification of the potential trends revealed by the seqMK (e.g., Bocchiola and Diolaiuti, 2010). The significance level is established for  $p < 0.05$ . We define a slight significance for  $p < 0.10$ . The uncertainty associated with the Sen's slopes (1994–2013) is estimated through a Monte Carlo uncertainty analysis (e.g., James and Oldenburg, 1997), described in detail in Supplement 1.

## 5 Results

### 5.1 Trend analysis at high elevation

Figure 3 shows the reconstructed PYRAMID time series for minT, maxT, meanT, and Prec resulting from the overall infilling process explained in Supplement 1. Figure 4 analyzes the monthly trends of  $T$  and Prec from 1994 to 2013 for PYRAMID.

#### 5.1.1 Minimum air temperature (minT)

November ( $0.17\text{ }^{\circ}\text{C a}^{-1}$ ,  $p < 0.01$ ) and December ( $0.21\text{ }^{\circ}\text{C a}^{-1}$ ,  $p < 0.01$ ) present the highest increasing trend, i.e., both these two months experienced about even  $+4\text{ }^{\circ}\text{C}$  over twenty years (Fig. 4a). In general, the post- and pre-monsoon periods experience higher and more significant increases than during the monsoon. In particular, we note the significant and consistent increase of April ( $0.10\text{ }^{\circ}\text{C a}^{-1}$ ,  $p < 0.05$ ). At the annual scale, the bottom graph shows a progressive  $\mu(\tau)$  trend parallel to the retrograde  $\mu(\tau)$  one for the entire analyzed period, i.e., a continuous tendency of minT to rise, which becomes significant in 2007, when the progressive  $\mu(\tau)$  assumes values above  $+1.96$ . On the right, the Sen's slope completes the analysis, illustrating that minT is increasing at annual level by  $0.072 \pm 0.011\text{ }^{\circ}\text{C a}^{-1}$ ,  $p < 0.001$ , i.e.,  $+1.44 \pm 0.22\text{ }^{\circ}\text{C}$  over twenty years.

#### 5.1.2 Maximum air temperature (maxT)

The post- and pre-monsoon months show larger increases in maxT, but with lower magnitudes and significance than we observe for minT (Fig. 4b). The highest increases occurs also for this variable in April, November and December. Less expected is the decrease of maxT in May ( $0.08\text{ }^{\circ}\text{C a}^{-1}$ ,  $p < 0.05$ ) and during the monsoon months from June to August ( $0.05\text{ }^{\circ}\text{C a}^{-1}$ ,  $p < 0.1$ ). On the annual scale, the bottom graph shows a continuous crossing of the progressive and retrograde  $\mu(\tau)$  trends until 2007, i.e., a general stationary condition. From 2007 until 2010, the trend significantly increased,

Title Page

Abstract

Introduction

Conclusions

References

Tables

Figures

◀

▶

◀

▶

Back

Close

Full Screen / Esc

Printer-friendly Version

Interactive Discussion



while 2012 and 2013 register a decrease, bringing the progressive  $\mu(\tau)$  near the stationary condition. In fact, on the right, the Sen's slope confirms that maxT is at annual level stationary over the twenty years ( $+0.009 \pm 0.012^\circ\text{C a}^{-1}$ ,  $p > 0.1$ ).

### 5.1.3 Mean air temperature (meanT)

Figure 4c, as expected, presents intermediate conditions for meanT than for minT and maxT. All months, except May and the monsoon months from June and August, register a positive trend (more or less significant). December presents the highest a more significant increasing trend ( $0.17^\circ\text{C a}^{-1}$ ,  $p < 0.01$ ), while April shows the highest and a more significant increase ( $p < 0.10$ ) during the pre-monsoon period. On the annual scale, the bottom graph shows that the progressive  $\mu(\tau)$  trend has always increased since 2000 and that it becomes significant beginning in 2008. On the right, the Sen's slope concludes this analysis, showing that meanT has been significantly increasing by  $0.044 \pm 0.008^\circ\text{C a}^{-1}$ ,  $p < 0.05$ , i.e.,  $+0.88 \pm 0.16^\circ\text{C}$  over twenty years.

### 5.1.4 Total precipitation (Prec)

In the last years, all cells are blue, i.e., we observe for all months an overall and strongly significant decreasing trend of Prec (Fig. 4d). In general, the post- and pre-monsoon periods experience more significant decreases, although the monsoon months (June–September) register the main Prec losses (e.g. August registers a Prec loss of even  $4.6\text{ mm a}^{-1}$ ). On the annual scale, the bottom graph shows a continuous decreasing progressive  $\mu(\tau)$  trend since 2000 that becomes significant beginning in 2005. On the right, the Sen's slope notes that the decreasing Prec trend is strongly high and significant at annual level ( $13.7 \pm 2.4\text{ mm a}^{-1}$ ,  $p < 0.001$ ).

The precipitation reduction is mainly due to a reduction in intensity. However during the early and late monsoon rather show a reduction in duration (see further details in Supplement 2).

## Weak precipitation, warm winters and springs impact glaciers of Mt. Everest

F. Salerno et al.

Title Page

Abstract

Introduction

Conclusions

References

Tables

Figures

◀

▶

◀

▶

Back

Close

Full Screen / Esc

Printer-friendly Version

Interactive Discussion



## 5.2 Trend analysis in the Koshi Basin

Table 2 provides the descriptive statistics of the Sen's slopes for minT, maxT, meanT, and Prec for the 1994–2013 period for the Koshi Basin. The stations located on the two sides of the Himalayan range are listed separately. For the southern ones (KO-S), we observe that for minT less than half of the stations experience an increasing trend and just three are significant with  $p < 0.1$ . In general, the minT on the southern side can be defined as stationary ( $+0.003^\circ\text{C a}^{-1}$ ). Conversely, the maxT shows a decidedly non-stationary condition. All stations present an increasing trend, and even six of the ten are on the significant rise with at least  $p < 0.1$ . The mean trend is  $+0.060^\circ\text{C a}^{-1}$  ( $p < 0.10$ ). Similarly, the meanT shows a substantial increase. Also in this case, six of the ten stations are on the significant rise with at least  $p < 0.1$ . The mean trend is  $+0.029^\circ\text{C a}^{-1}$  ( $p < 0.10$ ). In regards to Prec, we observe that on the KO-S, 14 of the 19 stations present a downward trend. Among them, eight decrease significantly with at least  $p < 0.1$ . The mean trend is  $-11.1\text{ mma}^{-1}$ , i.e., we observe a decreasing of 15% (222 mm) of precipitation fallen in the basin during the 1994–2013 period (1527 mm on average).

The two stations located on the northern ridge (KO-N) show a singularly slight significant rise for minT ( $0.034^\circ\text{C a}^{-1}$ ,  $p < 0.10$  on average) and for maxT ( $0.039^\circ\text{C a}^{-1}$ ,  $p < 0.10$  on average), recording a consequent mean increase of meanT equal to  $0.037^\circ\text{C a}^{-1}$ ,  $p < 0.05$ . As for Prec, we observe that on the KO-N both stations maintain stationary conditions ( $-0.1\text{ mma}^{-1}$ ).

Table 3 provides the descriptive statistics of the Sen's slopes on a seasonal base. The stations analyzed here are the same as those considered in Table 2. We begin our description with PYRAMID, already analyzed in detail in Fig. 4. We confirm with this seasonal grouping that the main and significant increases of minT, maxT, and meanT are completely concentrated during the post-monsoon period (e.g.,  $0.124^\circ\text{C a}^{-1}$ ,  $p < 0.01$  for meanT). The pre-monsoon period experienced a slighter and not significant increase (e.g.,  $0.035$ ,  $p > 0.1$  for meanT). In general, during the mon-

### Weak precipitation, warm winters and springs impact glaciers of Mt. Everest

F. Salerno et al.

Title Page

Abstract

Introduction

Conclusions

References

Tables

Figures

◀

▶

◀

▶

Back

Close

Full Screen / Esc

Printer-friendly Version

Interactive Discussion



## Weak precipitation, warm winters and springs impact glaciers of Mt. Everest

F. Salerno et al.

Title Page

Abstract

Introduction

Conclusions

References

Tables

Figures

◀

▶

◀

▶

Back

Close

Full Screen / Esc

Printer-friendly Version

Interactive Discussion

soon period,  $T$  is much more stationary for all three variables (e.g., 0.015,  $p > 0.1$  for mean $T$ ). Considering the other KO-S stations, the main increasing and significant trends of mean $T$  occurred during the pre-monsoon ( $0.043^{\circ}\text{C a}^{-1}$ ) and post-monsoon ( $0.030^{\circ}\text{C a}^{-1}$ ) season, while the increase during the monsoon is slighter ( $0.020^{\circ}\text{C a}^{-1}$ ).

The KO-N stations confirm that the main increasing trend of mean $T$  occurred outside the monsoon period that is stationary ( $+0.013^{\circ}\text{C a}^{-1}$ ).

As for Prec, PYRAMID and the other KO-S stations show that the magnitude of the Sen's slopes is higher during the monsoon season ( $-9.3\text{ mm a}^{-1}$  and  $-8.6\text{ mm a}^{-1}$ , respectively), when precipitation is more abundant. The relatively low snowfall phase of monsoon Prec at PYRAMID (as specified above) makes the decreasing trend observed during the summer more robust than the annual one as devoid of possible undervaluation of snowfall. The northern stations show slight significant decreasing Prec during the winter ( $-3.3\text{ mm a}^{-1}$ ,  $p < 0.05$ ).

### 5.3 Lapse rates in the southern Koshi Basin

#### 5.3.1 Air temperature gradient

This study, aiming to create a connection between the climate drivers and cryosphere in the Koshi Basin, which presents the highest altitudinal gradient of the world (77 to 8848 m a.s.l.), offers a unique opportunity to calculate  $T$  and Prec lapse rates before analyzing their spatial trends. It is worth noting that the  $T$  lapse rate is one of the most important variables for modeling meltwater runoff from a glacierized basin using the T-index method (Hock, 2005; Immerzeel et al., 2014). It is also an important variable for determining the form of Prec and its distribution characteristics (e.g., Hock, 2005). Figure 5a presents the lapse rate of the annual mean $T$  in the KO Basin (Nepal) along the altitudinal range of well over 7000 m (865 to 7986 m a.s.l.). We found an altitudinal gradient of  $-0.60^{\circ}\text{C (100 m)}^{-1}$  on the annual scale with a linear trend ( $r^2 = 0.98$ ,  $p < 0.001$ ). It is known that up to altitudes of approximately 8–17 km a.s.l. in the lower regions of the atmosphere,  $T$  decreases with altitude at a fairly uniform rate (Washing-

ton and Parkinson, 2005). Kattel and Yao (2013) recently found a lower annual lapse rate for the overall CH-S, but until 4000 m.a.s.l.:  $-0.52\text{ }^{\circ}\text{C (100 m)}^{-1}$ .

Considering that the lapse rate is mainly affected by the moisture content of the air (Washington and Parkinson, 2005), we also calculated the seasonal gradients (not shown here). We found a dry lapse rate of  $-0.65\text{ }^{\circ}\text{C (100 m)}^{-1}$  ( $r^2 = 0.99$ ,  $p < 0.001$ ) during the pre-monsoon season when AWS1 registers a mean relative humidity of 62%. A saturated lapse rate during the monsoon season is  $-0.57\text{ }^{\circ}\text{C (100 m)}^{-1}$  ( $r^2 = 0.99$ ,  $p < 0.001$ ) with a mean relative humidity of 96%. During the post-monsoon period, we found a lapse rate equal to that registered during the monsoon:  $-0.57\text{ (100 m)}^{-1}$  ( $r^2 = 0.98$ ,  $p < 0.001$ ) even if the relative humidity is decidedly lower in these months (44%). Kattel and Yao (2013) explain this anomalous low post-monsoon lapse rate as the effect of strong radiative cooling in winter.

### 5.3.2 Precipitation gradient

As for Prec, its relationship with elevation helps in providing a realistic assessment of water resources and hydrological modeling of mountainous regions (Barros et al., 2004). In recent years, the spatial variability of Prec has received attention because the mass losses of the Himalayan glaciers can be explained with an increased variability in the monsoon system (e.g., Yao et al., 2012; Thakuri et al., 2014). Some previous studies of the Himalayas have considered orographic effects on Prec (Singh and Kumar, 1997; Ichiyanagi et al., 2007). Ichiyanagi et al. (2007), using all available Prec stations operated by DHM, of which  $< 5\%$  of stations are located over 2500 m and just one station is over 4000 m.a.s.l., observed that in the CH-S region, the annual Prec increases with altitude below 2000 m.a.s.l. and decreases for elevations ranging between 2000 and 3500 m.a.s.l., but with no significant gradient. A broad picture of the relationship between Prec and topography in the Himalayas can be derived from the precipitation radar onboard the Tropical Rainfall Measuring Mission (TRMM). Some authors found an increasing trend with elevation characterized by two distinct maxima along two elevation bands (950 and 2100 m.a.s.l.). The second maximum is much higher than the

## Weak precipitation, warm winters and springs impact glaciers of Mt. Everest

F. Salerno et al.

Title Page

Abstract

Introduction

Conclusions

References

Tables

Figures

◀

▶

◀

▶

Back

Close

Full Screen / Esc

Printer-friendly Version

Interactive Discussion



first, and it is located along the Lesser Himalayas. Over these elevations, the annual distribution follows an approximate exponentially decreasing trend (Bookhagen and Burbank, 2006).

Figure 5b shows the altitudinal gradient for the total annual Prec in the Koshi Basin.

We observe a clear rise in Prec with elevation until approximately 2500 m a.s.l., corresponding to the Tarke Ghyang station (code 1058), registering an annual mean of 3669 mm (mean for the 2004–2012 period). A linear approximation ( $r = 0.83$ ,  $p < 0.001$ ) provides a rate of  $+1.16 \text{ mm m}^{-1}$ . At higher elevations, we observe an exponential decrease ( $ae^{bx}$ , with  $a = 21\,168 \text{ mm m}^{-1}$  and  $b = -9 \times 10^{-4} \text{ m}^{-1}$ , where  $x$  is the elevation expressed as m a.s.l.) until observing a minimum of 132 mm (years 2009 and 2013) for the Kala Patthar station (AWS4) at 5600 m a.s.l., although, as specified above, at these altitudes the contribution of winter snowfall could be underestimated. The changing point between the two gradients can be reasonably assumed at approximately 2500 m a.s.l., considering that the stations here present the highest interannual variability, belonging in this way, depending on the year, to the linear increase or to the exponential decrease. The clear outlier along the linear gradient is the Num Station (1301) located at 1497 m a.s.l., which recorded 4608 mm of precipitation. This station has been excluded for the linear approximation because, as reported by Montgomery and Stolar (2006), the station is located in the Arun Valley, which acts as a conduit for northward transport of monsoonal precipitation. The result is that local precipitation within the gorge of the Arun River is several times greater than in surrounding areas.

#### 5.4 Spatial distribution of air temperature and precipitation trends in the Koshi Basin

Figure 6 presents the spatial distribution of the Sen's slopes in the Koshi Basin for minT (Fig. 6a), maxT (Fig. 6b), meanT (Fig. 6c), and Prec (Fig. 6d) during the 1994–2013 period. The relevant data are reported in Table 2. The Chainpur (East) station shows  $T$  trends in contrast with the other stations (see also Table 2); therefore, we consider this station as a local anomaly and do not discuss it further in the following sections.

### Weak precipitation, warm winters and springs impact glaciers of Mt. Everest

F. Salerno et al.

Title Page

Abstract

Introduction

Conclusions

References

Tables

Figures

◀

▶

◀

▶

Back

Close

Full Screen / Esc

Printer-friendly Version

Interactive Discussion





## Weak precipitation, warm winters and springs impact glaciers of Mt. Everest

F. Salerno et al.

Title Page

Abstract

Introduction

Conclusions

References

Tables

Figures

◀

▶

◀

▶

Back

Close

Full Screen / Esc

Printer-friendly Version

Interactive Discussion



In regards to minT, we observe an overall stationary condition in KO-S, as noted above. The only two stations showing a significant increasing trend are both located at East. The high elevation stations (PYRAMID and both those located on the north ridge) differ from the general pattern of the southern basin by showing a significant increasing trend. Even for maxT, we observe a higher increase in the southeastern basin. The central and western parts of the KO-S seem to be more stationary. PYRAMID follows this stationary pattern, while the northern stations (KO-N) show large and significant increases. As a consequence, meanT shows increasing trends for all the Koshi Basin, especially on the southeast and northern sides.

The decrease of precipitation in the southern Koshi Basin presents a quite homogeneous pattern from which the highly elevated PYRAMID is not excluded. The pattern is different on the north ridge, where it is stationary.

## 6 Discussion

### 6.1 Temperature trends of the Koshi Basin compared to the regional pattern

Kattel and Yao (2013) analyzed the annual minT, maxT, and meanT trends from stations ranging from 1304 to 2566 m a.s.l. in CH-S (corresponding to all stations in Nepal) during the 1980–2009 period. They found that the magnitude of warming is higher for maxT ( $0.065\text{ }^{\circ}\text{C a}^{-1}$ ), while minT ( $0.011\text{ }^{\circ}\text{C a}^{-1}$ ) exhibits larger variability, such as positive, negative or no change; meanT was found to increase at an intermediate rate of  $0.038\text{ }^{\circ}\text{C a}^{-1}$ . These authors extended some time series and confirmed the findings of Shrestha et al. (1999) that, analyzing the 1971–1994 period, found a maxT increase of  $0.059\text{ }^{\circ}\text{C a}^{-1}$  for all of Nepal. Furthermore, warming in the winter was more pronounced compared to other seasons in both studies. These results are consistent with the pattern reported in WH (e.g., Bhutiyani et al., 2007; Shekhar et al., 2010), in EH, and in the rest of India (e.g., Pal and Al-Tabbaa, 2010) for the last three decades.

## Weak precipitation, warm winters and springs impact glaciers of Mt. Everest

F. Salerno et al.

Title Page

Abstract

Introduction

Conclusions

References

Tables

Figures

◀

▶

◀

▶

Back

Close

Full Screen / Esc

Printer-friendly Version

Interactive Discussion

The trend analysis carried out in this study for the last two decades in KO-S shows full consistency with the pattern of change occurring in these regions over the last three decades in terms of a higher increase in maxT ( $0.060^{\circ}\text{C a}^{-1}$ ) than in minT ( $0.003^{\circ}\text{C a}^{-1}$ ), a seasonal pattern (more pronounced during the pre- and post-monsoon months), and the magnitudes of the trends (e.g., the meanT trend is  $+0.030^{\circ}\text{C a}^{-1}$ ). Therefore, at low elevations of KO-S, we observe an acceleration of warming in the recent years compared to the rate of change reported by Kattel and Yao (2013) and Shrestha et al. (1999) in the previous decades.

Different conditions have been observed on the TP, where the warming of minT is more prominent than that of maxT (e.g., Liu et al., 2006, 2009). In particular, for stations above 2000 m a.s.l. during the 1961–2003 period, Liu et al. (2006) found that minT trends were consistently greater ( $+0.041^{\circ}\text{C a}^{-1}$ ) than those of maxT ( $+0.018^{\circ}\text{C a}^{-1}$ ), especially in the winter and spring months. Yang et al. (2012), focusing their analysis on CH-N (which corresponds to the southern TP) in a more recent period (1971–2007), showed a significant increase of  $0.031^{\circ}\text{C a}^{-1}$  for meanT. Yang et al. (2006) analyzed five stations located in a more limited area of CH-N: the northern side of Mt. Everest (therefore, including the two stations also considered in this study) from 1971 to 2004. The warming is observed to be influenced more markedly by the minT increase.

The trend analysis carried out in this study for KO-N over the last two decades agrees with these studies in regards to both the considerable increase of minT ( $0.034^{\circ}\text{C a}^{-1}$ ) and the seasonal consistency of trends, related to all three  $T$  variables, outside the monsoon months. However, we observe that in recent years, maxT is increasing more than the rest of the TP ( $0.039^{\circ}\text{C a}^{-1}$ ). In general we observed an increase of meanT ( $0.037^{\circ}\text{C a}^{-1}$ ) comparable to that reported by Yang et al. (2012) ( $0.031^{\circ}\text{C a}^{-1}$ ) in the 1971–2007 period.

With all these regional studies, PYRAMID shares the higher  $T$  trends outside the monsoon period. However, in contrast with studies located south of the Himalayan ridge, which observed a prevalence of maxT increase, PYRAMID experienced a consistent minT increase ( $0.072^{\circ}\text{C a}^{-1}$  for PYRAMID vs.  $0.003^{\circ}\text{C a}^{-1}$  for KO-S sta-

tions), while the maxT increase is decidedly weaker ( $0.009^{\circ}\text{C a}^{-1}$  for PYRAMID vs.  $0.060^{\circ}\text{C a}^{-1}$  for KO-S stations). The remarkable minT trend of PYRAMID is higher, but more similar to the pattern of change commonly described on the TP, in particular in CH-N, and also in this study ( $0.072^{\circ}\text{C a}^{-1}$  for PYRAMID vs.  $0.034^{\circ}\text{C a}^{-1}$  for KO-N stations), while the maxT increase is weaker ( $0.009^{\circ}\text{C a}^{-1}$  for PYRAMID vs.  $0.039^{\circ}\text{C a}^{-1}$  for KO-N stations).

## 6.2 Elevation dependency of temperature trends

Figure 7 shows  $T$  trends in the KO Basin for minT, meanT, and maxT relative to the elevation during the 1994–2013 period. No linear pattern emerges. However, we can observe the minT trend of the three stations located at higher altitude (PYRAMID and KO-N stations), which increases more than that of the lower stations (Fig. 7a, see also Table 2). Reviewing the most recent studies in the surroundings, we found that they are quite exclusively located on CH-N. These studies often show contradictory elevation dependencies (Rangwala and Miller, 2012). A recent study by You et al. (2010) did not find any significant elevation dependency in the warming rates of meanT between 1961 and 2005. However, considering mostly the same stations, Liu et al. (2009) found that the warming rates for minT were greater at higher elevations. Observations from CH-S are much rarer. Shrestha et al. (1999) found elevation dependency in the rate at which maxT were increasing in the Nepali Himalayas (CH-S), with higher rates at higher elevations, but this study exclusively considered stations under 3000 m a.s.l.

Furthermore we did not find for the Koshi Basin any significant elevation dependency in the weakening rates of Prec.

## 6.3 Precipitation trends of the Koshi Basin compared to the regional pattern

Turner and Annamalai (2012), using the all-India rainfall data based on a weighted mean of 306 stations, observed a negative precipitation trend since the 1950s in South Asia. According to Yao et al. (2012), using the Global Precipitation Climatology Project

### Weak precipitation, warm winters and springs impact glaciers of Mt. Everest

F. Salerno et al.

Title Page

Abstract

Introduction

Conclusions

References

Tables

Figures

◀

▶

◀

▶

Back

Close

Full Screen / Esc

Printer-friendly Version

Interactive Discussion



**Weak precipitation,  
warm winters and  
springs impact  
glaciers of  
Mt. Everest**

F. Salerno et al.

[Title Page](#)[Abstract](#)[Introduction](#)[Conclusions](#)[References](#)[Tables](#)[Figures](#)[◀](#)[▶](#)[◀](#)[▶](#)[Back](#)[Close](#)[Full Screen / Esc](#)[Printer-friendly Version](#)[Interactive Discussion](#)

(GPCP) data, there is strong evidence that precipitation from 1979 to 2010 decreased even in the Himalayas. In eastern CH-S, where the Koshi Basin is located, they estimated a loss of 173 mm, showing a real decreasing trend starting from the early 1990s (mean value between grid 9 and 11 in Fig. S18 of their paper).

On the TP, the observed pattern of change is opposite that of the monsoon weakening described by the authors cited above. Liu et al. (2010) described an increase in precipitation in CH-N for the period of the 1980s to 2008. Su et al. (2006) described a marked precipitation increase in the Yangtze River Basin (eastern CH-N). In a similar way to the  $T$  analysis, Yang et al. (2006) considered 5 stations located on the northern side of Mt. Everest (therefore, including the two stations also considered in this study) from 1971 to 2004 and observed an increasing, but not significant Prec trend. The higher stationarity we observed is confirmed since 1971 for the two KO-N stations considered in this study.

Different from the north side of Mt. Everest and from the general TP, we confirm the general monsoon weakening in the KO-S, observing a substantial Prec decrease of 15% ( $-11.1 \text{ mm a}^{-1}$ , 222 mm), but that is not significant for all stations. At PYRAMID, the annual loss is relatively comparable with that of the KO-S ( $13.7 \text{ mm a}^{-1}$ , 273 mm), but at these high elevations, as we observed in Table 2, the weather is much more drier (449 and 1527 mm, respectively). Therefore, the fractional loss is more than 3 times (52%) that of the KO-S. Considering that the decreasing trend observed during the summer is more robust than the annual one (see above), the fractional loss of Prec during the monsoon is 47%, which means that currently, on average, the precipitation at PYRAMID is the half of what it was twenty years ago.

#### 6.4 Mechanisms responsible for temperature warming and precipitation weakening

According to Rangwala and Miller (2012), there are a number of mechanisms that can cause enhanced warming rates at high elevation, and they often have strong seasonal dependency. These mechanisms arise from either elevation based differential changes

## Weak precipitation, warm winters and springs impact glaciers of Mt. Everest

F. Salerno et al.

Title Page

Abstract

Introduction

Conclusions

References

Tables

Figures

◀

▶

◀

▶

Back

Close

Full Screen / Esc

Printer-friendly Version

Interactive Discussion

in climate drivers, such as snow cover, clouds, specific humidity, aerosols, and soil moisture, or differential sensitivities of surface warming to changes in these drivers at different elevations. This study does not aim to either realize a comprehensive review or to demonstrate the causes that could have led to the climate change pattern observed at PYRAMID, but our intent here is just to note the recent hypotheses advanced in the literature that fit with our observations for the region of investigation.

Snow/ice albedo is one of the strongest feedbacks in the climate system (Rangwala and Miller, 2012). Increases in minT are possible if decreases in snow cover are accompanied by increases in soil moisture and surface humidity, which can facilitate a greater diurnal retention of the daytime solar energy in the land surface and amplify the longwave heating of the land surface at night (Rangwala et al., 2012). For the Tibetan Plateau, Rikiishi and Nakasato (2006) found that the length of the snow cover season declined at all elevations between 1966 and 2001. Moreover, minT can be enhanced by nighttime increases in cloud cover. However, assessing changes in clouds and quantifying cloud feedbacks will remain challenging in the near term. For the Tibetan Plateau, Duan and Wu (2006) found that low level nocturnal cloud cover increased over the TP between 1961 and 2003 and that these increases explain part of the observed increases in minT.

The maxT increase observed here during April ( $p < 0.05$  in 2011, Fig. 4b) fits with the warming reported by Pal and Al-Tabbaa (2010) which observed that within the pre-monsoon season only April shows significant changes in maxT in all Indian regions and WH (1901–2003 period). According to Ramanathan et al. (2007), Gautam et al. (2010) argued that the observed warming during the pre-monsoon period (April–June) can be ascribed not only to the global greenhouse warming, but also to the solar radiation absorption caused by the large amount of aerosol (mineral dust mixed with other carbonaceous material) transported over the Gangetic-Himalayan region. As recently reported by Marinoni et al. (2013), April represents the month for which the transport of absorbing carbonaceous aerosol (i.e. black carbon) is maximized in our region of investigation (Khumbu Valley). At this regards Putero et al. (2013) show evidences for

## Weak precipitation, warm winters and springs impact glaciers of Mt. Everest

F. Salerno et al.

Title Page

Abstract

Introduction

Conclusions

References

Tables

Figures

◀

▶

◀

▶

Back

Close

Full Screen / Esc

Printer-friendly Version

Interactive Discussion



a possible influence of open fire occurrence in South Asia particular abundant during this period of the year. However the significant decreasing of maxT observed in May ( $p < 0.05$ ) and the slight significant decreasing during the monsoon months from June to August ( $p < 0.10$ ) appear to deviate from the scenario proposed for April. In this respect it should be kept in mind that the radioactive dynamical interactions of aerosol with the monsoon cycle are extremely complex and different processes can interact with each other. As an instance, as reported by Qian et al. (2011), the deposition of absorbing aerosol on snow and the snow albedo feedback processes can play a prominent role in Himalayas and TP inducing large radioactive flux changes and surface temperature perturbation.

Recent studies associate the precipitation decrease over India during the second half of 20th century (e.g., Ramanathan et al., 2005; Lau and Kim, 2006) to the significant tropospheric warming over the tropical area from the Indian Ocean to the western Pacific (e.g., Wu, 2005), while westerlies are strengthening (Zhao et al., 2012). Other authors (e.g., Bollasina et al., 2011) attribute the monsoon weakening to human-influenced aerosol emissions. In fact an increase of aerosols over South Asia has been well documented (Ramanathan et al., 2005; Lau and Kim, 2006) and climate model experiments suggest that sulfate aerosol may significantly reduce monsoon precipitation (Mitchell and Johns, 1997). Despite a historical weakening of the monsoon circulation, most studies project an increase of the seasonal monsoon rainfall under global warming. At this regards Levy II et al., 2013 find that the dramatic emission reductions (35–80 %) in anthropogenic aerosols and their precursors projected by Representative Concentration Pathway (RCP) 4.5 (Moss et al., 2010) result an increasing trend by the second half of the 21st century in South Asia and in particular over the Himalaya (Palazzi et al., 2013).

## 6.5 Linking climate change patterns observed at high elevation with glacier responses

### 6.5.1 Impact of temperature increase

Air temperature and precipitation are the two factors most commonly related to glacier fluctuations. However, there still exists a seasonal gap in order to explain the shrinking of summer accumulation-type glaciers (typical of CH) due to large temperature increases observed in the region during winter (Ueno and Aryal, 2008), as is the case for the south slopes of Mt. Everest. Furthermore, in this study we noted a slightly significant decline in summer maxT and stationary meanT. The real increase of  $T$  has been observed for minT, but given the mean elevation of glaciers (5695 m a.s.l. in 1992) and the mean elevation range of glacier fronts (4568–4817 m a.s.l. in 1992, mean 4817 m a.s.l., 249 m of SD) (Thakuri et al., 2014), this increase for minT can be most likely considered ineffective for melting processes, since  $T$  is still less than  $0^{\circ}\text{C}$ . This inference can be ascertained analyzing Fig. 8, created in order to link temperature increases and altitudinal glacier distribution (data from Thakuri et al., 2014). The  $0^{\circ}\text{C}$  isotherms, corresponding to the mean monthly minT and maxT, are plotted for 1994 and 2013. The elevation of each  $0^{\circ}\text{C}$  isotherm is calculated according to the accurate lapse rates computation carried out in this study and the observed monthly  $T$  trends. We can note that in 1994 the  $0^{\circ}\text{C}$  isotherm for minT reached the elevation band characterizing the glacier fronts only from June to September. However, twenty years later, the upward of the  $0^{\circ}\text{C}$  isotherm is modest (92 m) during these months, compared to the huge but ineffective rise for melting processes (downstream from the glacier fronts) of December–November (even 854 m). The maxT has obviously a greater potential impact on glaciers. In fact the  $0^{\circ}\text{C}$  isotherm for of all months except January and February crosses the elevation bands within which the glacier fronts are located ever since 1994. In this regard we observe that only April (224 m), December (212 m), and November (160 m) experienced an upward of the  $0^{\circ}\text{C}$  isotherm able to enhance the melting processes, but only close to the glaciers fronts. We therefore point out that the impact caused by the increased tem-

## Weak precipitation, warm winters and springs impact glaciers of Mt. Everest

F. Salerno et al.

Title Page

Abstract

Introduction

Conclusions

References

Tables

Figures

◀

▶

◀

▶

Back

Close

Full Screen / Esc

Printer-friendly Version

Interactive Discussion





perature occurring in April most likely plays an important role not only in relation to this case study, but also at the level of the Himalayan range. In fact, as mentioned above, Pal and Al-Tabbaa (2010), observed that within the pre-monsoon season, only April showed significant changes in maxT in all Indian regions and WH (1901–2003 period).

### 6.5.2 Impact of precipitation decrease

As regards the precipitation, in this study we noted a strong and significant decreasing Prec trend for all months, corresponding to a fractional loss of 47 % during the monsoon season which indicates that, on average, the precipitation at PYRAMID is currently half of what it was twenty years ago. This climate change pattern confirms and clarifies the observation of Thakuri et al. (2014), who noted that the southern Mt. Everest glaciers experienced a shrinkage acceleration over the last twenty years (1992–2011), as underlined by an upward shift of SLA with a velocity almost three times greater than the previous period (1962–1992). The authors, without the support of climatic data, proposed the hypothesis that Mt. Everest glaciers are shrinking faster since the early 1990s mainly as a result of a weakening of precipitation over the last decades. In fact they observed a double upward shift in the SLA of the largest glaciers (south-oriented and with a higher altitude accumulation zone): a clear signal of a significant decrease in accumulation. Wagnon et al. (2013) have recently reached the same conclusion, but also in this case without the support of any climatic studies. Bolch et al. (2011) and Nuimura et al. (2012) registered a higher mass loss rate during the last decade (2000–2010).

Furthermore Quincey et al. (2009) and Peters et al. (2010) observed lower glacier flow velocity in the region over the last decades. Many studies highlight how the present condition of ice stagnation of glaciers in the Mt Everest region, and in general in CH-S, is attributable to low flow velocity generated by generally negative mass balances (Bolch et al., 2008; Quincey et al., 2009; Scherler et al., 2011). Our observations allow attributing the lower glacier flow velocity to lower accumulation due to weaker precipitation, which can thus be considered the main climatic factor driving the current ice

## Weak precipitation, warm winters and springs impact glaciers of Mt. Everest

F. Salerno et al.

Title Page

Abstract

Introduction

Conclusions

References

Tables

Figures

◀

▶

◀

▶

Back

Close

Full Screen / Esc

Printer-friendly Version

Interactive Discussion



stagnation of tongues. In this regard we need to keep in mind that changes in velocity are among the main triggers for the formation of supraglacial and proglacial lakes (Salerno et al., 2012; Quincey et al., 2009), which we know to be susceptible to GLOFs.

### 6.5.3 Trend analysis of annual probability of snowfall

Figure 9 analyses how the changes observed for the meanT at PYRAMID have affected the probability of snowfall on total cumulated annual precipitation in the last twenty years. The increase of meanT observed outside the monsoon period, when the precipitation is almost completely composed by snow (Fig. 2), brought a significant decrease of solid phase ( $0.7\% \text{ a}^{-1}$ ,  $p < 0.05$ ). Extending this analysis to the elevation bands characterizing the glaciers distribution (see Fig. 8), through the temperature lapse rate calculated here, we observe that at the level of the mean glaciers (5695 m.a.s.l.) the probability of snowfall is stationary ( $+0.04\% \text{ a}^{-1}$ ), while it decreases at the mean elevation of SLAs (5345 m.a.s.l. in 1992, Thakuri et al., 2014), but not significantly ( $-0.38\% \text{ a}^{-1}$ ,  $p > 0.1$ ). The reduction becomes significant at lower altitudes. In particular, at the mean elevation of glacier fronts (4817 m.a.s.l.) the probability of snowfall is  $-0.56\% \text{ a}^{-1}$  ( $p < 0.05$ ), i.e. at these altitudes the probability of snow on annual base is currently 11% ( $p < 0.05$ ) less than twenty years ago. We can conclude this analysis summarizing that a significant change in precipitation phase has occurred close to the terminal portions of glaciers, corresponding broadly to the glaciers ablation zones (around 10%,  $p < 0.5$ ), while the lower temperature of the upper glaciers zones has so far guaranteed a stationary condition.

## 7 Conclusion

Most relevant studies on temperature trends were conducted on the Tibetan Plateau, the Indian subcontinent (including the WH) and the Upper Indus Basin, while studies on the mountainous regions along the southern slope of the central Himalayas in Nepal

## Weak precipitation, warm winters and springs impact glaciers of Mt. Everest

F. Salerno et al.

Title Page

Abstract

Introduction

Conclusions

References

Tables

Figures

◀

▶

◀

▶

Back

Close

Full Screen / Esc

Printer-friendly Version

Interactive Discussion

(CH-S) are limited. Although Shrestha et al. (1999) analyzed the maximum temperature trends over Nepal during the period 1971–1994, studies on recent temperature trends over CH-S are still lacking and, before this study, completely absent as regards high elevation. This paper addresses seasonal variability of minimum, maximum, and mean temperatures and precipitation at high elevation on the southern slopes of Mt. Everest. Moreover, we complete this analysis with data from all the existing weather stations located on both sides of the Himalayan range (Koshi Basin) for the 1994–2013 period, during which a rapider glacier mass loss occurred.

At high elevation on the southern slopes of Mt. Everest, we observed the following:

1. The main increases in air temperature are almost completely concentrated during the post-monsoon months. The pre-monsoon period experienced a slighter and insignificant increase, while the monsoon season is generally stationary. This seasonal temperature change pattern is shared with the entire Koshi Basin, and it is also observed in the regional studies related to the northern and southern slopes of the Himalayan range. Surprisingly, at high elevation the maximum temperature decreases significantly in May and slightly during the monsoon months from June to August.
2. The minimum temperature increased much more than the maximum temperature. This remarkable minimum temperature trend is more similar to the pattern of change commonly described on the Tibetan Plateau and confirmed in this study in the northern Koshi Basin. However, this trend is in contrast with studies located south of the Himalayan ridge. As proved by this study, the southern Koshi Basin experienced a prevalence of maximum temperature increases. No linear pattern emerges in the elevation dependency of temperature trends. We only observed higher minimum temperature trends at higher altitudes.
3. The total annual precipitation has considerably decreased. The annual rate of decrease at high elevation is similar to the one at lower altitudes on the southern side of the Koshi Basin, but the drier conditions of this remote environment make

## Weak precipitation, warm winters and springs impact glaciers of Mt. Everest

F. Salerno et al.

Title Page

Abstract

Introduction

Conclusions

References

Tables

Figures

◀

▶

◀

▶

Back

Close

Full Screen / Esc

Printer-friendly Version

Interactive Discussion



the fractional loss relatively more consistent. The precipitation at high elevation during the monsoon period is currently half of what it was twenty years ago. These observations confirm the monsoon weakening observed by previous studies in India and even in the Himalayas since the early 1980s. As opposed to the northern side of the Koshi Basin that shows in this study certain stability, as positive or stationary trends have been observed by previous studies on the TP and more specifically in northern central Himalaya.

4. There is a significantly lower probability of snowfall in the glaciers ablation zones, while the lower temperature of the upper glaciers zones have so far guaranteed a stationary condition.

In general, this study contributes to change the perspective on how the climatic driver (temperature vs. precipitation) led the glacier responses in the last twenty years. to a change perspective related to the climatic driver (temperature vs. precipitation) led the glacier responses in the last twenty years.

Without demonstrating the causes that could have led to the climate change pattern observed at the PYRAMID, we simply note the recent literature on hypotheses that accord with our observations. for the case study.

In conclusion, we have here observed that weather stations at low elevations are not able to suitably describe the climate changes occurring at high altitudes and thus correctly interpret the impact observed on the cryosphere. This consideration stresses the great importance of long-term ground measurements at high elevation.

**The Supplement related to this article is available online at doi:10.5194/tcd-8-5911-2014-supplement.**

*Author contributions.* G. Tartari, Y. Ma and E. Vuillermoz designed research; F. Salerno performed research; F. Salerno, N. Guyennon, S. Thakuri, G. Viviano and E. Romano analyzed data; F. Salerno, N. Guyennon, E. Romano and G. Tartari wrote the paper. P. Cristofanelli, P. Stocchi, N. Guyennon and G. Agrillo data quality check.

5 *Acknowledgements.* This work was supported by the MIUR through Ev-K2-CNR/SHARE and CNR-DTA/NEXTDATA project within the framework of the Ev-K2-CNR and Nepal Academy of Science and Technology (NAST). Sudeep Thakuri is recipient of the IPCC Scholarship Award under the collaboration between the IPCC Scholarship Programme and the Prince Albert II of Monaco Foundation's Young Researchers Scholarships Initiative.

## 10 References

Abebe, A., Solomatine, D., and Venneker, R.: Application of adaptive fuzzy rule based models for reconstruction of missing precipitation events, *Hydrolog. Sci. J.*, 45, 425–436, doi:10.1080/02626660009492339, 2000.

15 Abudu, S., Bawazir, A. S., and King, J. P.: Infilling missing daily evapotranspiration data using neural networks, *J. Irrig. Drain. E.-ASCE*, 136, 317–325, doi:10.1061/(ASCE)IR.1943-4774.0000197, 2010.

Amatya, L. K., Cuccillato, E., Haack, B., Shadie, P., Sattar, N., Bajracharya, B., Shrestha, B., Caroli, P., Panzeri, D., Basani, M., Schommer, B., Flury, B. Salerno, F., and Manfredi, E. C.: Improving communication for management of social-ecological systems in high mountain areas: development of methodologies and tools – the HKKH Partnership Project, *Mt. Res. Dev.*, 30, 69–79, doi:10.1659/MRD-JOURNAL-D-09-00084.1, 2010.

20 Bajracharya, B., Uddin, K., Chettri, N., Shrestha, B., and Siddiqui, S. A.: Understanding land cover change using a harmonized classification system in the Himalayas: a case study from Sagarmatha National Park, Nepal, *Mt. Res. Dev.*, 30, 143–156, doi:10.1659/MRD-JOURNAL-D-09-00044.1, 2010.

25 Barros, A. P., Kim, G., Williams, E., and Nesbitt, S. W.: Probing orographic controls in the Himalayas during the monsoon using satellite imagery, *Nat. Hazards Earth Syst. Sci.*, 4, 29–51, doi:10.5194/nhess-4-29-2004, 2004.

30 Benn, D. I., Bolch, T., Hands, K., Gullely, J., Luckman, A., Nicholson, L. I., Quincey, D., Thompson, S., Toumi, R., and Wiseman, S.: Response of debris-covered glaciers in the Mount

### Weak precipitation, warm winters and springs impact glaciers of Mt. Everest

F. Salerno et al.

Title Page

Abstract

Introduction

Conclusions

References

Tables

Figures

◀

▶

◀

▶

Back

Close

Full Screen / Esc

Printer-friendly Version

Interactive Discussion



## Weak precipitation, warm winters and springs impact glaciers of Mt. Everest

F. Salerno et al.

Title Page

Abstract

Introduction

Conclusions

References

Tables

Figures

◀

▶

◀

▶

Back

Close

Full Screen / Esc

Printer-friendly Version

Interactive Discussion



Everest region to recent warming, and implications for outburst flood hazards, *Earth-Sci. Rev.*, 114, 156–174, doi:10.1016/j.earscirev.2012.03.008, 2012.

Bertolani, L., Bollasina, M., and Tartari, G.: Recent biannual variability of meteorological features in the eastern Highland Himalayas, *Geophys. Res. Lett.*, 27, 2185–2188, doi:10.1029/1999GL011198, 2000.

Bhutiyani, M. R., Kale, V. S., and Pawar, N. J.: Long-term trends in maximum, minimum and mean annual air temperatures across the Northwestern Himalaya during the twentieth century, *Climatic Change*, 85, 159–177, doi:10.1007/s10584-006-9196-1, 2007.

Bocchiola, D. and Diolaiuti, G.: Evidence of climate change within the Adamello Glacier of Italy, *Theor. Appl. Climatol.*, 100, 351–369, doi:10.1007/s00704-009-0186-x, 2010.

Bolch, T., Buchroithner, M., Pieczonka, T., and Kunert, A.: Planimetric and volumetric glacier changes in the Khumbu Himal, Nepal, since 1962 using Corona, Landsat TM and ASTER data, *J. Glaciol.*, 54, 592–600, doi:10.3189/002214308786570782, 2008.

Bolch, T., Pieczonka, T., and Benn, D. I.: Multi-decadal mass loss of glaciers in the Everest area (Nepal Himalaya) derived from stereo imagery, *The Cryosphere*, 5, 349–358, doi:10.5194/tc-5-349-2011, 2011.

Bolch, T., Kulkarni, A., Kääb, A., Huggel, C., Paul, F., Cogley, J. G., Frey, H., Kargel, J. S., Fujita, K., Scheel, M., Bajracharya, S., and Stoffel, M.: The state and fate of Himalayan glaciers, *Science*, 336, 310–314, doi:10.1126/science.1215828, 2012.

Bollasina, M. A., Ming, Y., and Ramaswamy, V.: Anthropogenic aerosols and the weakening of the south Asian summer monsoon, *Science*, 334, 502–505, doi:10.1126/science.1204994, 2011.

Bookhagen, B. and Burbank, D. W.: Topography, relief, and TRMM-derived rainfall variations along the Himalaya, *Geophys. Res. Lett.*, 33, L08405, doi:10.1029/2006GL026037, 2006.

Carraro, E., Guyennon, N., Hamilton, D., Valsecchi, L., Manfredi, E. C., Viviano, G., Salerno, F., Tartari, G., and Copetti, D.: Coupling high-resolution measurements to a three-dimensional lake model to assess the spatial and temporal dynamics of the cyanobacterium *Planktothrix rubescens* in a medium-sized lake, *Hydrobiologia*, 698, 77–95, doi:10.1007/s10750-012-1096-y, 2012a.

Carraro, E., Guyennon, N., Viviano, G., Manfredi, E. C., Valsecchi, L., Salerno, F., Tartari, G., and Copetti, D.: Impact of global and local pressures on the ecology of a medium-sized pre-alpine lake, in: *Models of the Ecological Hierarchy*, edited by: Jordan, F. and Jorgensen, S. E., Elsevier, 259–274, doi:10.1016/B978-0-444-59396-2.00016-X, 2012b.

**Weak precipitation,  
warm winters and  
springs impact  
glaciers of  
Mt. Everest**

F. Salerno et al.

Title Page

Abstract

Introduction

Conclusions

References

Tables

Figures

◀

▶

◀

▶

Back

Close

Full Screen / Esc

Printer-friendly Version

Interactive Discussion



- Coulibaly, P. and Evora, N.: Comparison of neural network methods for infilling missing daily weather records, *J. Hydrol.*, 341, 27–41, doi:10.1016/j.jhydrol.2007.04.020, 2007.
- Déqué, M.: Frequency of precipitation and temperature extremes over France in an anthropogenic scenario: model results and statistical correction according to observed values, *Global Planet. Change*, 57, 16–26, doi:10.1016/j.gloplacha.2006.11.030, 2007.
- Duan, A. and Wu, G.: Change of cloud amount and the climate warming on the Tibetan Plateau, *Geophys. Res. Lett.*, 33, L22704, doi:10.1029/2006GL027946, 2006.
- Dytham, C.: *Choosing and Using Statistics: a Biologist's Guide*, John Wiley & Sons, New York, USA, 2011.
- Fujita, K. and Sakai, A.: Modelling runoff from a Himalayan debris-covered glacier, *Hydrol. Earth Syst. Sci.*, 18, 2679–2694, doi:10.5194/hess-18-2679-2014, 2014.
- Fujita, K., Sakai, A., Takenaka, S., Nuimura, T., Surazakov, A. B., Sawagaki, T., and Yamanokuchi, T.: Potential flood volume of Himalayan glacial lakes, *Nat. Hazards Earth Syst. Sci.*, 13, 1827–1839, doi:10.5194/nhess-13-1827-2013, 2013.
- Ganguly, N. D. and Iyer, K. N.: Long-term variations of surface air temperature during summer in India, *Int. J. Climatol.*, 29, 735–746, doi:10.1002/joc.1748, 2009.
- Gardelle, J., Arnaud, Y., and Berthier, E.: Contrasted evolution of glacial lakes along the Hindu Kush Himalaya mountain range between 1990 and 2009, *Global Planet. Change*, 75, 47–55, doi:10.1016/j.gloplacha.2010.10.003, 2011.
- Gautam, R., Hsu, N. C., and Lau, K. M.: Premonsoon aerosol characterization and radiative effects over the Indo-Gangetic plains: implications for regional climate warming, *J. Geophys. Res.*, 115, D17208, doi:10.1029/2010JD013819, 2010.
- Gerstengarbe, F. W. and Werner, P. C.: Estimation of the beginning and end of recurrent events within a climate regime, *Clim. Res.*, 11, 97–107, 1999.
- Guyennon, N., Romano, E., Portoghese, I., Salerno, F., Calmanti, S., Petrangeli, A. B., Tartari, G., and Copetti, D.: Benefits from using combined dynamical-statistical downscaling approaches – lessons from a case study in the Mediterranean region, *Hydrol. Earth Syst. Sci.*, 17, 705–720, doi:10.5194/hess-17-705-2013, 2013.
- Hock, R.: Glacier melt: a review of processes and their modeling, *Prog. Phys. Geog.*, 29, 362–391, doi:10.1191/0309133305pp453ra, 2005.
- Ichayanagi, K., Yamanaka, M. D., Muraji, Y., and Vaidya, B. K.: Precipitation in Nepal between 1987 and 1996, *Int. J. Climatol.*, 27, 1753–1762, doi:10.1002/joc.1492, 2007.



**Weak precipitation,  
warm winters and  
springs impact  
glaciers of  
Mt. Everest**

F. Salerno et al.

Title Page

Abstract

Introduction

Conclusions

References

Tables

Figures

◀

▶

◀

▶

Back

Close

Full Screen / Esc

Printer-friendly Version

Interactive Discussion

Immerzeel, W. W., Petersen, L., Ragetti, S., and Pellicciotti, F.: The importance of observed gradients of air temperature and precipitation for modeling runoff from a glacierized watershed in the Nepal Himalayas, *Water Resour. Res.*, 50, 2212–2226, doi:10.1002/2013WR014506, 2014.

James, A. L. and Oldenburg, C. M.: Linear and Monte Carlo uncertainty analysis for subsurface contaminant transport simulation, *Water Resour. Res.*, 33, 2495–2508, doi:10.1029/97WR01925, 1997.

Kattel, D. B. and Yao, T.: Recent temperature trends at mountain stations on the southern slope of the central Himalayas, *J. Earth Syst. Sci.*, 122, 215–227, doi:10.1007/s12040-012-0257-8, 2013.

Kendall, M. G.: *Rank Correlation Methods*, Oxford University Press, New York, 1975.

Kivekäs, N., Sun, J., Zhan, M., Kerminen, V.-M., Hyvärinen, A., Komppula, M., Viisanen, Y., Hong, N., Zhang, Y., Kulmala, M., Zhang, X.-C., Deli-Geer, and Lihavainen, H.: Long term particle size distribution measurements at Mount Waliguan, a high-altitude site in inland China, *Atmos. Chem. Phys.*, 9, 5461–5474, doi:10.5194/acp-9-5461-2009, 2009.

Lami, A., Marchetto, A., Musazzi, S., Salerno, F., Tartari, G., Guilizzoni, P., Rogora, M., and Tartari, G. A.: Chemical and biological response of two small lakes in the Khumbu Valley, Himalayas (Nepal) to short-term variability and climatic change as detected by long-term monitoring and paleolimnological methods, *Hydrobiologia*, 648, 189–205, doi:10.1007/s10750-010-0262-3, 2010.

Lau, K.-M. and Kim, K.-M.: Observational relationships between aerosol and Asian monsoon rainfall, and circulation, *Geophys. Res. Lett.*, 33, L21810, doi:10.1029/2006GL027546, 2006.

Lavagnini, I., Badocco, D., Pastore, P., and Magno, F.: Theil-Sen nonparametric regression technique on univariate calibration, inverse regression and detection limits, *Talanta*, 87, 180–188, doi:10.1016/j.talanta.2011.09.059, 2011.

Levy II, H., Horowitz, L. W., Schwarzkopf, M. D., Ming, Y., Golaz, J. C., Naik, V., and Ramaswamy, V.: The roles of aerosol direct and indirect effects in past and future climate change, *J. Geophys. Res.*, 118, 1–12, doi:10.1002/jgrd.50192, 2013.

Liu, J., Yang, B., and Qin, C.: Tree-ring based annual precipitation reconstruction since AD 1480 in south central Tibet, *Quatern. Int.*, 236, 75–81, doi:10.1016/j.quaint.2010.03.020, 2010.

Liu, K., Cheng, Z., Yan, L., and Yin, Z.: Elevation dependency of recent and future minimum surface air temperature trends in the Tibetan Plateau and its surroundings, *Global Planet. Change*, 68, 164–174, doi:10.1016/j.gloplacha.2009.03.017, 2009.

**Weak precipitation,  
warm winters and  
springs impact  
glaciers of  
Mt. Everest**

F. Salerno et al.

Title Page

Abstract

Introduction

Conclusions

References

Tables

Figures

◀

▶

◀

▶

Back

Close

Full Screen / Esc

Printer-friendly Version

Interactive Discussion

- Liu, X. D. and Chen, B. D.: Climatic warming in the Tibetan Plateau during recent decades, *Int. J. Climatol.*, 20, 1729–1742, doi:10.1002/1097-0088(20001130)20:14<1729::AID-JOC556>3.0.CO;2-Y, 2000.
- Liu, X. D., Yin, Z. Y., Shao, X., and Qin, N.: Temporal trends and variability of daily maximum and minimum, extreme temperature events, and growing season length over the eastern and central Tibetan Plateau during 1961–2003, *J. Geophys. Res.*, 111, D19109, doi:10.1029/2005JD006915, 2006.
- Manfredi, E. C., Flury, B., Viviano, G., Thakuri, S., Khanal, S. N., Jha, P. K., Maskey, R. K., Kayastha, R. B., Kafle, K. R., Bhochohibhoya, S., Ghimire, N. P., Shrestha, B. B., Chaudhary, G., Giannino, F., Carteni, F., Mazzoleni, S., and Salerno, F.: Solid waste and water quality management models for Sagarmatha National Park and Buffer Zone, Nepal: implementation of a participatory modeling framework, *Mt. Res. Dev.*, 30, 127–142, doi:10.1659/MRD-JOURNAL-D-10-00028.1, 2010.
- Marinoni, A., Cristofanelli, P., Laj, P., Putero, D., Calzolari, F., Landi, T. C., Vuillermoz, E., Maione, M., and Bonasoni, P.: High black carbon and ozone concentrations during pollution transport in the Himalayas: five years of continuous observations at NCO-Prec global GAW station, *J. Environ. Sci.*, 25, 1618–1625, doi:10.1016/S1001-0742(12)60242-3, 2013.
- Mitchell, J. F. B. and Johns, T. C.: On the modification of global warming by sulphate aerosols, *J. Climate*, 10, 245–267, 1997.
- Montgomery, D. R. and Stolar, D. B.: Reconsidering Himalayan river anticlines, *Geomorphology*, 82, 4–15, doi:10.1016/j.geomorph.2005.08.021, 2006.
- Moss, R. H., Edmonds, J. A., Hibbard, K. A., Manning, M. R., Rose, S. K., van Vuuren, D. P., Carter, T. R., Emori, S., Kainuma, M., Kram, T., Meehl, G. A., Mitchell, J. F. B., Nakicenovic, N., Riahi, K., Smith, S. J., Stouffer, R. J., Thomson, A. M., Weyant, J. P., and Wilbanks, T. J.: The next generation of scenarios for climate change research and assessment, *Nature*, 463, 747–756, doi:10.1038/nature08823, 2010.
- Nuimura, T., Fujita, K., Yamaguchi, S., and Sharma, R. R.: Elevation changes of glaciers revealed by multitemporal digital elevation models calibrated by GPS survey in the Khumbu region, Nepal Himalaya, 1992–2008, *J. Glaciol.*, 58, 648–656, doi:10.3189/2012JoG11J061, 2012.
- Pal, I. and Al-Tabbaa, A.: Long-term changes and variability of monthly extreme temperatures in India, *Theor. Appl. Climatol.*, 100, 45–56, doi:10.1007/s00704-009-0167-0, 2010.

**Weak precipitation,  
warm winters and  
springs impact  
glaciers of  
Mt. Everest**

F. Salerno et al.

Title Page

Abstract

Introduction

Conclusions

References

Tables

Figures

◀

▶

◀

▶

Back

Close

Full Screen / Esc

Printer-friendly Version

Interactive Discussion



Palazzi, E., von Hardenberg, J., and Provenzale, A.: Precipitation in the Hindu-Kush Karakoram Himalaya: observations and future scenarios, *J. Geophys. Res.-Atmos.*, 118, 85–100, doi:10.1029/2012JD018697, 2013.

Pepin, N. C. and Lundquist, J. D.: Temperature trends at high elevations: patterns across the globe, *Geophys. Res. Lett.*, 35, L14701, doi:10.1029/2008GL034026, 2008.

Peters, J., Bolch, T., Buchroithner, M. F., and Bäßler, M.: Glacier Surface Velocities in the Mount Everest Area/Nepal using ASTER and Ikonos imagery, in: *Proceeding of 10th International Symposium on High Mountain Remote Sensing Cartography*, Kathmandu, Nepal, 8–11 September 2008, 313–320, 2010.

Putero, D., Landi, T. C., Cristofanelli, P., Marinoni, A., Laj, P., Duchi, R., Calzolari, F., Verza, G. P., and Bonasoni, P.: Influence of open vegetation fires on black carbon and ozone variability in the southern Himalayas (NCO-P, 5079 m.a.s.l.), *Environ. Pollut.*, 184, 597–604, doi:10.1016/j.envpol.2013.09.035, 2013.

Qian, Y., Flanner, M. G., Leung, L. R., and Wang, W.: Sensitivity studies on the impacts of Tibetan Plateau snowpack pollution on the Asian hydrological cycle and monsoon climate, *Atmos. Chem. Phys.*, 11, 1929–1948, doi:10.5194/acp-11-1929-2011, 2011.

Quincey, D. J., Luckman, A., and Benn, D.: Quantification of Everest region glacier velocities between 1992 and 2002, using satellite radar interferometry and feature tracking, *J. Glaciol.*, 55, 596–606, doi:10.3189/002214309789470987, 2009.

Ramanathan, V., Chung, C., Kim, D., Bettge, T., Buja, L., Kiehl, J. T., Washington, W. M., Fu, Q., Sikka, D. R., and Wild, M.: Atmospheric brown clouds: impacts on South Asian climate and hydrological cycle, *P. Natl. Acad. Sci. USA*, 102, 5326–5333, doi:10.1073/pnas.0500656102, 2005.

Ramanathan, V., Li, F., Ramana, M. V., Praveen, P. S., Kim, D., Corrigan, C. E., Nguyen, H., Stone, E. A., Schauer, J. J., Carmichael, G. R., Adhikary, B., and Yoon, S. C.: Atmospheric brown clouds: hemispherical and regional variations in long-range transport, absorption, and radiative forcing, *J. Geophys. Res.*, 112, D22S21, doi:10.1029/2006JD008124, 2007.

Rangwala, I. and Miller, J. R.: Climate change in mountains: a review of elevation-dependent warming and its possible causes, *Climatic Change*, 114, 527–547, doi:10.1007/s10584-012-0419-3, 2012.

Rangwala, I., Barsugli, J., Cozzetto, K., Neff, J., and Prairie, J.: Mid-21st century projections in temperature extremes in the southern Colorado Rocky Mountains from regional climate models, *Clim. Dynam.*, 39, 1823–1840, doi:10.1007/s00382-011-1282-z, 2012.

**Weak precipitation,  
warm winters and  
springs impact  
glaciers of  
Mt. Everest**

F. Salerno et al.

Title Page

Abstract

Introduction

Conclusions

References

Tables

Figures

◀

▶

◀

▶

Back

Close

Full Screen / Esc

Printer-friendly Version

Interactive Discussion



Rikiishi, K. and Nakasato, H.: Height dependence of the tendency for reduction in seasonal snow cover in the Himalaya and the Tibetan Plateau region, 1966–2001, *Ann. Glaciol.*, 43, 369–377, doi:10.3189/172756406781811989, 2006.

Salerno, F., Buraschi, E., Bruccoleri, G., Tartari, G., and Smiraglia, C.: Glacier surface-area changes in Sagarmatha National Park, Nepal, in the second half of the 20th century, by comparison of historical maps, *J. Glaciol.*, 54, 738–752, 2008.

Salerno, F., Thakuri, S., D'Agata, C., Smiraglia, C., Manfredi, E. C., Viviano, G., and Tartari, G.: Glacial lake distribution in the Mount Everest region: uncertainty of measurement and conditions of formation, *Global Planet. Change*, 92–93, 30–39, doi:10.1016/j.gloplacha.2012.04.001, 2012.

Salerno, F., Viviano, G., Mangredi, E. C., Caroli, P., Thakuri, S., and Tartari, G.: Multiple Carrying Capacities from a management-oriented perspective to operationalize sustainable tourism in protected area, *J. Environ. Manage.*, 128, 116–125, doi:10.1016/j.jenvman.2013.04.043, 2013.

Salerno, F., Gambelli, S., Viviano, G., Thakuri, S., Guyennon, N., D'Agata, C., Diolaiuti, G., Smiraglia, C., Stefani, F., Bochhiola, D., and Tartari, G.: High alpine ponds shift upwards as average temperature increase: a case study of the Ortles-Cevedale mountain group (Southern alps, Italy) over the last 50 years, *Global Planet. Change*, 120, 81–91, doi:10.1016/j.gloplacha.2014.06.003, 2014.

Scherler, D., Bookhagen, B., and Strecker, M. R.: Spatially variable response of Himalayan glaciers to climate change affected by debris cover, *Nature Geosci.*, 4, 156–159, doi:10.1038/ngeo1068, 2011.

Schneider, T.: Analysis of incomplete climate data: estimation of mean values and covariance matrices and imputation of missing values, *J. Climate*, 14, 853–871, doi:10.1175/1520-0442(2001)014<0853:AOICDE>2.0.CO;2, 2001.

Sellegrì, K., Laj, P., Venzac, H., Boulon, J., Picard, D., Villani, P., Bonasoni, P., Marinoni, A., Cristofanelli, P., and Vuillermoz, E.: Seasonal variations of aerosol size distributions based on long-term measurements at the high altitude Himalayan site of Nepal Climate Observatory-Pyramid (5079 m), Nepal, *Atmos. Chem. Phys.*, 10, 10679–10690, doi:10.5194/acp-10-10679-2010, 2010.

Sen, P. K.: Estimates of the regression coefficient based on Kendall's Tau, *J. Am. Stat. Assoc.*, 63, 1379–1389, doi:10.2307/2285891, 1968.



**Weak precipitation,  
warm winters and  
springs impact  
glaciers of  
Mt. Everest**

F. Salerno et al.

Title Page

Abstract

Introduction

Conclusions

References

Tables

Figures

◀

▶

◀

▶

Back

Close

Full Screen / Esc

Printer-friendly Version

Interactive Discussion



Ueno, K. and Aryal, R.: Impact of tropical convective activity on monthly temperature variability during non monsoon season in the Nepal Himalayas, *J. Geophys. Res.*, 113, D18112, doi:10.1029/2007JD009524, 2008.

Ueno, K., Endoh, N., Ohata, T., Yabuki, H., Koike, M., and Zhang, Y.: Characteristics of precipitation distribution in Tangula, Monsoon, 1993, *B. Glaciol. Res.*, 12, 39–46, 1994.

UNEP (United Nations Environment Programme)/WCMC (World Conservation Monitoring Centre): Sagarmatha National Park, Nepal, in: *Encyclopedia of Earth*, edited by: McGinley, M., and Cleveland, C. J., Environmental Information Coalition, National Council for Science and the Environment, Washington, DC, available at: <http://www.eoearth.org/view/article/155820> (last access: 28 November 2014), 2008.

Venzac, H., Sellegri, K., Laj, P., Villani, P., Bonasoni, P., Marinoni, A., Cristofanelli, P., Calzolari, F., Fuzzi, S., Decesari, S., Facchini, M. C., Vullermoz, E., and Verza, G. P.: High frequency new particle formation in the Himalayas, *P. Natl. Acad. Sci. USA*, 105, 15666–15671, doi:10.1073/pnas.0801355105, 2008.

Vuille, M.: Climate variability and high altitude temperature and precipitation, in: *Encyclopedia of Snow, Ice and Glaciers*, edited by: Singh, V. P., Singh, P., and Haritashya, U. K., Springer, the Netherlands, 153–156, 2011.

Wagnon, P., Vincent, C., Arnaud, Y., Berthier, E., Vuillermoz, E., Gruber, S., Ménégoz, M., Gilbert, A., Dumont, M., Shea, J. M., Stumm, D., and Pokhrel, B. K.: Seasonal and annual mass balances of Mera and Pokalde glaciers (Nepal Himalaya) since 2007, *The Cryosphere*, 7, 1769–1786, doi:10.5194/tc-7-1769-2013, 2013.

Washington, W. M. and Parkinson, C. L.: *An Introduction to Three-Dimensional Climate Modeling*, 2nd edn., University Science Books, Sausalito, 2005.

Wu, B.: Weakening of Indian summer monsoon in recent decades, *Adv. Atmos. Sci.*, 22, 21–29, doi:10.1007/BF02930866, 2005.

Yang, J., Tan, C., and Zhang, T.: Spatial and temporal variations in air temperature and precipitation in the Chinese Himalayas during the 1971–2007, *Int. J. Climatol.*, 33, 2622–2632, doi:10.1002/joc.3609, 2012.

Yang, X., Zhang, Y., Zhang, W., Yan, Y., Wang, Z., Ding, M., and Chu, D.: Climate change in Mt. Qomolangma region since 1971, *J. Geogr. Sci.*, 16, 326–336, doi:10.1007/s11442-006-0308-7, 2006.

Yao, T., Thompson, L., Yang, W., Yu, W., Gao, Y., Guo, X., Yang, X., Duan, K., Zhao, H., Xu, B., Pu, J., Lu, A., Xiang, Y., Kattel, D. B., and Joswiak, D.: Different glacier status with atmo-

spheric circulations in Tibetan Plateau and surroundings, Nat. Clim. Change, 2, 663–667, doi:10.1038/nclimate1580, 2012.

You, Q., Kang, S., Pepin, N., Flügel, W., Yan, Y., Behrawan, H., and Huang, J.: Relationship between temperature trend magnitude, elevation and mean temperature in the Tibetan Plateau from homogenized surface stations and reanalysis data, Global Planet. Change, 71, 124–133, doi:10.1016/j.gloplacha.2010.01.020, 2010.

Zhao, H., Xu, B., Yao, T., Wu, G., Lin, S., Gao, J., and Wang, M.: Deuterium excess record in a southern Tibetan ice core and its potential climatic implications, Clim. Dynam., 38, 1791–1803, doi:10.1007/s00382-011-1161-7, 2012.

TCD

8, 5911–5959, 2014

**Weak precipitation, warm winters and springs impact glaciers of Mt. Everest**

F. Salerno et al.

Title Page

Abstract

Introduction

Conclusions

References

Tables

Figures

◀

▶

◀

▶

Back

Close

Full Screen / Esc

Printer-friendly Version

Interactive Discussion





## Weak precipitation, warm winters and springs impact glaciers of Mt. Everest

F. Salerno et al.

**Table 1.** List of surface stations belonging to PYRAMID Observatory Laboratory network located along the south slopes of Mt. Everest (upper DK Basin).

Station ID	Location	Latitude °N	Longitude °E	Elevation m a.s.l.	Sampling Frequency	Data Availability		% of daily missing data	
						From	To	Air Temperature	Precipitation
AWS3	Lukla	27.70	86.72	2660	1 h	2 Nov 2004	31 Dec 2012	23	20
AWSN	Namche	27.80	86.71	3570	1 h	27 Oct 2001	31 Dec 2012	21	27
AWS2	Pheriche	27.90	86.82	4260	1 h	25 Oct 2001	31 Dec 2013	15	22
AWS0	Pyramid	27.96	86.81	5035	2 h	1 Jan 1994	31 Dec 2005	19	16
AWS1	Pyramid	27.96	86.81	5035	1 h	1 Jan 2000	31 Dec 2013	10	21
ABC	Pyramid	27.96	86.82	5079	1 h	1 Mar 2006	31 Dec 2011	5	1
AWS4	Kala Patthar	27.99	86.83	5600	10 min	1 Jan 2009	31 Dec 2013	28	38
AWS5	South Col	27.96	86.93	7986	10 min	1 May 2008	31 Oct 2011	39	100

Title Page

Abstract

Introduction

Conclusions

References

Tables

Figures

◀

▶

◀

▶

Back

Close

Full Screen / Esc

Printer-friendly Version

Interactive Discussion

**Weak precipitation,  
warm winters and  
springs impact  
glaciers of  
Mt. Everest**

F. Salerno et al.

**Table 2.** List of ground weather stations located in the Koshi Basin and descriptive statistics of the Sen’s slopes for minimum, maximum, and mean air temperatures and total precipitation for the 1994–2012 period. The annual mean air temperature, the total annual mean precipitation, and the percentage of missing daily values is also reported.

ID	Station Name	Latitude °N	Longitude °N	Elevation m a.s.l.	Air Temperature					Precipitation		
					Annual mean °C	Missing values %	MinT trend °C a <sup>-1</sup>	MaxT trend °C a <sup>-1</sup>	MeanT trend °C a <sup>-1</sup>	Annual total mm	Missing values %	Prec trend mm a <sup>-1</sup>
1024	DHULIKHEL	27.61	85.55	1552	17.1	2	-0.012	0.041	0.026			
1036	PANCHKHAL	27.68	85.63	865	21.4	10	0.038	0.051 <sup>b</sup>	0.038 <sup>a</sup>	1191	10	-25.0 <sup>b</sup>
1058	TARKE GHYANG	28.00	85.55	2480						3669	10	-21.9
1101	NAGDAHA	27.68	86.10	850						1369	3	-1.4
1103	JIRI	27.63	86.23	2003	14.4	1	0.013	0.020	0.014 <sup>a</sup>	2484	4	6.6
1202	CHAURIKHARK	27.70	86.71	2619						2148	2	1.3
1206	OKHALDHUNGA	27.31	86.50	1720	17.6	2	-0.017	0.042	0.000	1786	3	-5.1
1210	KURULE GHAT	27.13	86.41	497						1017	2	-23.4 <sup>a</sup>
1211	KHOTANG BAZAR	27.03	86.83	1295						1324	4	15.9
1222	DIKTEL	27.21	86.80	1623						1402	6	10.4
1301	NUM	27.55	87.28	1497						4537	6	-54.3 <sup>c</sup>
1303	CHAINPUR (EAST)	27.28	87.33	1329	19.1	0	-0.127 <sup>b</sup>	0.024	-0.064 <sup>a</sup>	1469	0	-1.1
1304	PAKHTRIBAS	27.05	87.28	1680	16.7	0	-0.005	0.036 <sup>b</sup>	0.015	1540	4	-3.7
1307	DHANKUTA	26.98	87.35	1210	20.0	0	-0.002	0.153 <sup>d</sup>	0.071 <sup>d</sup>	942	6	-9.2 <sup>a</sup>
1314	TERHATHUM	27.13	87.55	1633	18.2	10	0.033	0.066 <sup>a</sup>	0.049 <sup>b</sup>	1052	6	-13.1 <sup>a</sup>
1317	CHEPUWA	27.46	87.25	2590						2531	5	-41.9 <sup>b</sup>
1322	MACHUWAGHAT	26.96	87.16	158						1429	6	-22.9 <sup>a</sup>
1403	LUNGTHUNG	27.55	87.78	1780						2347	1	2.6
1405	TAPLEJUNG	27.35	87.66	1732	16.6	1	0.060 <sup>b</sup>	0.085 <sup>c</sup>	0.071 <sup>c</sup>	1966	3	-11.6
1419	PHIDIM	27.15	87.75	1205	21.2	7	0.047 <sup>b</sup>	0.082 <sup>c</sup>	0.067 <sup>c</sup>	1287	2	-13.6 <sup>b</sup>
	MEAN	27.33	87.00	1587	17.9	2	0.003	0.060 <sup>a</sup>	0.029 <sup>a</sup>	1527	4	-11.1
	PYRAMID	27.96	86.81	5035	-2.4	0	0.072 <sup>d</sup>	0.009	0.044 <sup>b</sup>	449	0	-13.7 <sup>d</sup>
KO-N (TIBET)	DINGRI	28.63	87.08	4.302	3.5	0	0.037 <sup>a</sup>	0.041 <sup>a</sup>	0.037 <sup>b</sup>	309	0	-0.1
	NYALAM	28.18	85.97	3.811	4.1	0	0.032 <sup>a</sup>	0.036 <sup>a</sup>	0.036 <sup>a</sup>	616	0	-0.2
	MEAN	28.41	86.53	4.057	3.8	0.1	0.034 <sup>a</sup>	0.039 <sup>a</sup>	0.037 <sup>b</sup>	463	0	-0.1

Level of significance (<sup>a</sup>  $p$  value = 0.1, <sup>b</sup>  $p$  value = 0.05, <sup>c</sup>  $p$  value = 0.01, and <sup>d</sup>  $p$  value = 0.001).

Title Page

Abstract Introduction

Conclusions References

Tables Figures

◀ ▶

◀ ▶

Back Close

Full Screen / Esc

Printer-friendly Version

Interactive Discussion



## Weak precipitation, warm winters and springs impact glaciers of Mt. Everest

F. Salerno et al.

**Table 3.** Descriptive statistics of the Sen's slopes on a seasonal basis for minimum, maximum, and mean air temperatures and total precipitation of weather stations located in the Koshi Basin for the 1994–2012 period. The Nepali and Tibetan stations are aggregated as mean values.

Location	Minimum Temperature				Maximum Temperature				Mean Temperature				Total Precipitation			
	Pre-	Monsoon	Post-	Annual	Pre-	Monsoon	Post-	Annual	Pre-	Monsoon	Post-	Annual	Pre-	Monsoon	Post-	Annual
SOUTHERN KOSHI BASIN (KO-S, NEPAL)	0.012	-0.005	-0.001	0.003	0.076 <sup>a</sup>	0.052	0.069 <sup>a</sup>	0.060 <sup>a</sup>	0.043	0.020	0.030	0.030 <sup>a</sup>	0.8	-8.6	-2.5	-11.1
PYRAMID (NEPAL)	0.067 <sup>a</sup>	0.041 <sup>a</sup>	0.151 <sup>d</sup>	0.072 <sup>d</sup>	0.024	-0.028	0.049	0.009	0.035	0.015	0.124 <sup>c</sup>	0.044 <sup>c</sup>	-2.5 <sup>c</sup>	-9.3 <sup>c</sup>	-1.4 <sup>c</sup>	-13.7 <sup>d</sup>
NORTHERN KOSHI BASIN (KO-N, TIBET)	0.042 <sup>a</sup>	0.019	0.086 <sup>b</sup>	0.034 <sup>a</sup>	0.023	0.030	0.071 <sup>b</sup>	0.039 <sup>a</sup>	0.042 <sup>a</sup>	0.013	0.084 <sup>b</sup>	0.037 <sup>b</sup>	2.2	0.4	-3.3 <sup>b</sup>	-0.1

Level of significance (<sup>a</sup>  $p$  value = 0.1, <sup>b</sup>  $p$  value = 0.05, <sup>c</sup>  $p$  value = 0.01, and <sup>d</sup>  $p$  value = 0.001). Annual and seasonal temperature trends are expressed as  $^{\circ}\text{C a}^{-1}$ . Annual precipitation trend is expressed as  $\text{mm a}^{-1}$ , while the seasonal precipitation trends are in  $\text{mm (4 months) a}^{-1}$ .

[Title Page](#)
[Abstract](#)
[Introduction](#)
[Conclusions](#)
[References](#)
[Tables](#)
[Figures](#)
[Back](#)
[Close](#)
[Full Screen / Esc](#)
[Printer-friendly Version](#)
[Interactive Discussion](#)


## Weak precipitation, warm winters and springs impact glaciers of Mt. Everest

F. Salerno et al.

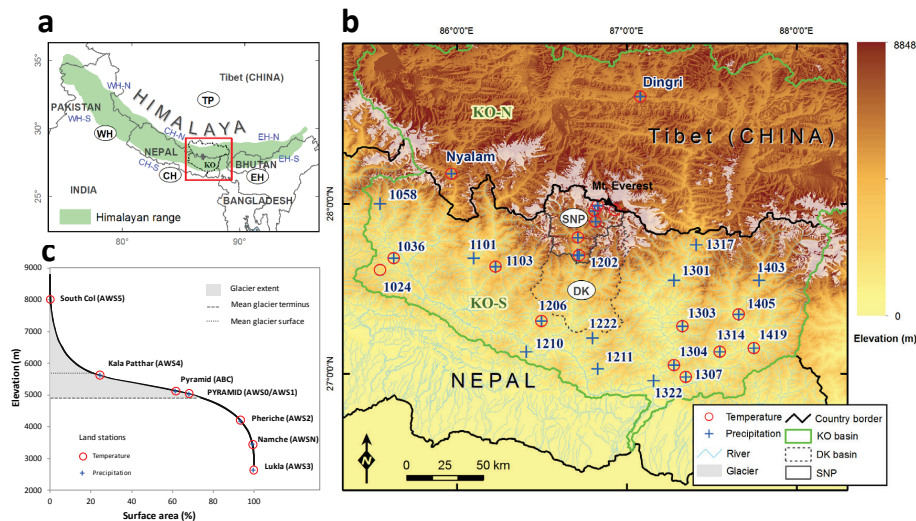


**Figure 1.** (a) Location of the study area in the Himalaya, where the abbreviations WH, CH, EH represents the Western, Central and Eastern Himalaya, respectively (the suffixes -N and -S indicate the northern and southern slopes). (b) Focused map on the spatial distribution of all meteorological stations used in this study, where KO and DK stand for the Koshi and Dudh Koshi Basins, respectively; SNP represents the Sagarmatha National Park. (c) Hypsometric curve of SNP (upper DK Basin) and altitudinal glacier distribution. Along this curve, the locations of meteorological stations belonging to PYRAMID Observatory Laboratory are presented.

Title Page

Abstract

Introduction

Conclusions

References

Tables

Figures

◀

▶

◀

▶

Back

Close

Full Screen / Esc

Printer-friendly Version

Interactive Discussion

## Weak precipitation, warm winters and springs impact glaciers of Mt. Everest

F. Salerno et al.

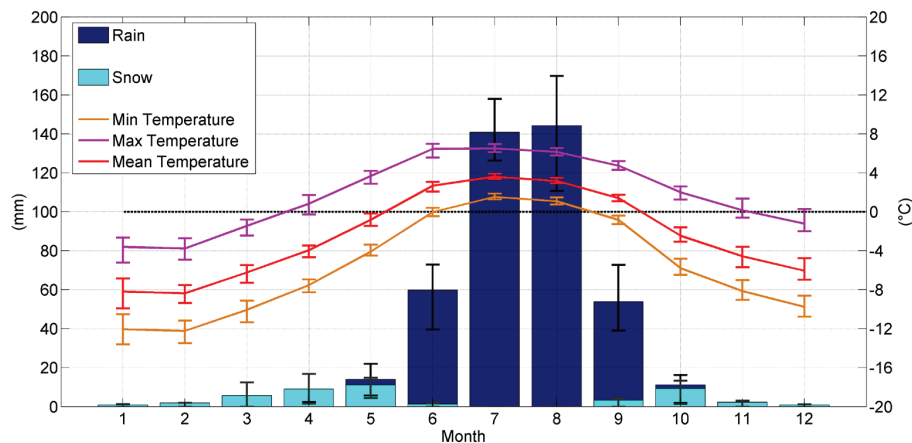


**Figure 2.** Mean monthly cumulated precipitation subdivided into snowfall and rainfall and minimum, maximum, and mean temperature at 5050 m a.s.l. (reference period 1994–2013). The bars represent the SD.

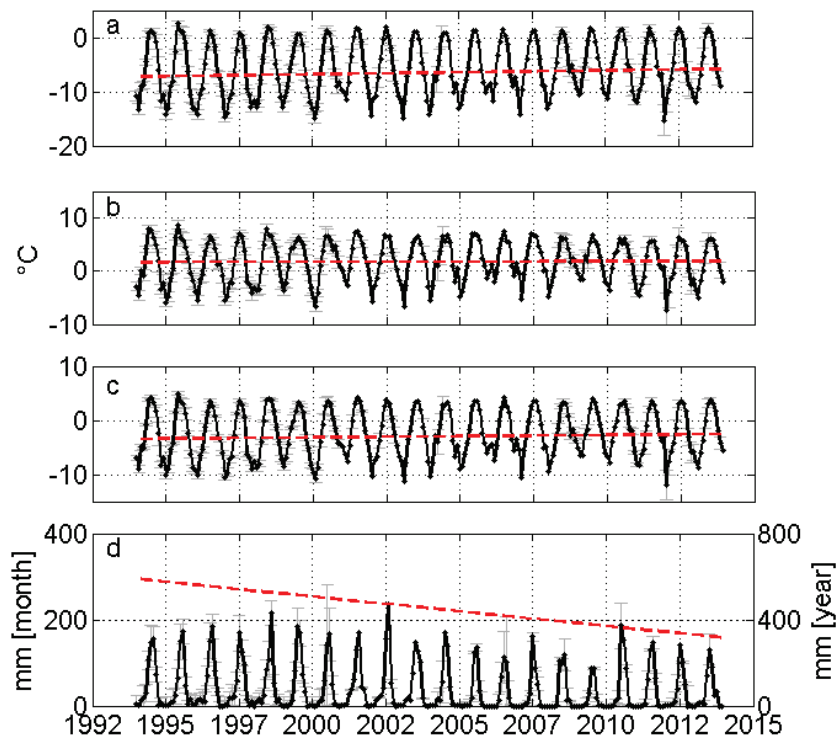


**Figure 3.** Temperature and precipitation monthly time series (1994–2013) reconstructed at high elevations of Mt. Everest (PYRAMID): minimum (a), maximum (b), and mean temperature (c), and precipitation (d). Uncertainty at 95 % is presented as gray bar. The red lines represents the robust linear fitting of the time series characterized by the associated Sen's slope. According to Dytham (2011), the intercepts are calculated by taking the slopes back from every observation to the origin. The intercepts used in here represent the median values of the intercepts calculated for every point (Lavagnini et al., 2011). For precipitation the linear fitting refers at the right axis.

**Weak precipitation, warm winters and springs impact glaciers of Mt. Everest**

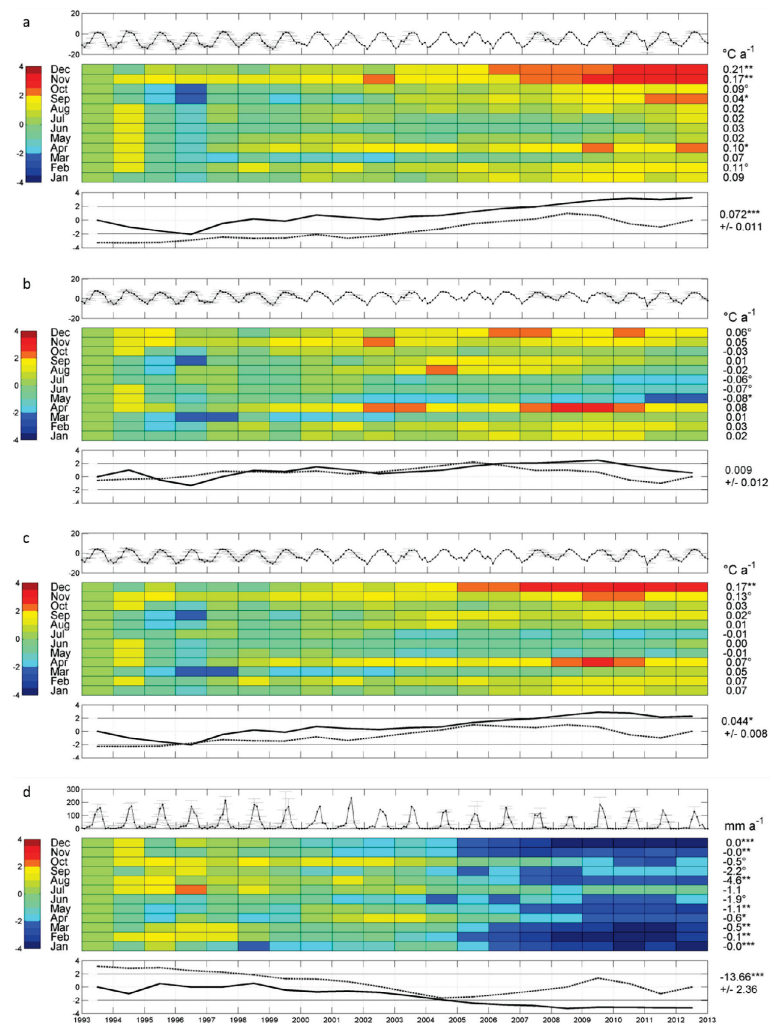
F. Salerno et al.

Title Page	
Abstract	Introduction
Conclusions	References
Tables	Figures
◀	▶
◀	▶
Back	Close
Full Screen / Esc	
Printer-friendly Version	
Interactive Discussion	



## Weak precipitation, warm winters and springs impact glaciers of Mt. Everest

F. Salerno et al.



Title Page

Abstract Introduction

Conclusions References

Tables Figures

◀ ▶

◀ ▶

Back Close

Full Screen / Esc

Printer-friendly Version

Interactive Discussion





**Figure 4.** Trend analysis for (a) minimum, (b) maximum, and (c) mean air temperatures and (d) total precipitation in the upper DK Basin. The top graph of each meteorological variable shows the monthly trend (dark line) and uncertainty due to the reconstruction process (gray bars). The central grid displays the results of the sequential Mann–Kendall (seqMK) test applied at the monthly level. On the left, the color bar represents the normalized Kendall's tau coefficient  $\mu(\tau)$ . The color tones below  $-1.96$  and above  $1.96$  are significant ( $\alpha = 5\%$ ). On the right, the monthly Sen's slopes and the relevant significance levels for the 1994–2013 period ( $^{\circ}$   $p$  value =  $0.1$ ,  $^*$   $p$  value =  $0.05$ ,  $^{**}$   $p$  value =  $0.01$ , and  $^{***}$   $p$  value =  $0.001$ ). The bottom graph plots the progressive (black line) and retrograde (dotted line)  $\mu(\tau)$  applied on the annual scale. On the right, the annual Sen's slope is shown for the 1994–2013 period.

## Weak precipitation, warm winters and springs impact glaciers of Mt. Everest

F. Salerno et al.

Title Page

Abstract

Introduction

Conclusions

References

Tables

Figures

◀

▶

◀

▶

Back

Close

Full Screen / Esc

Printer-friendly Version

Interactive Discussion

## Weak precipitation, warm winters and springs impact glaciers of Mt. Everest

F. Salerno et al.

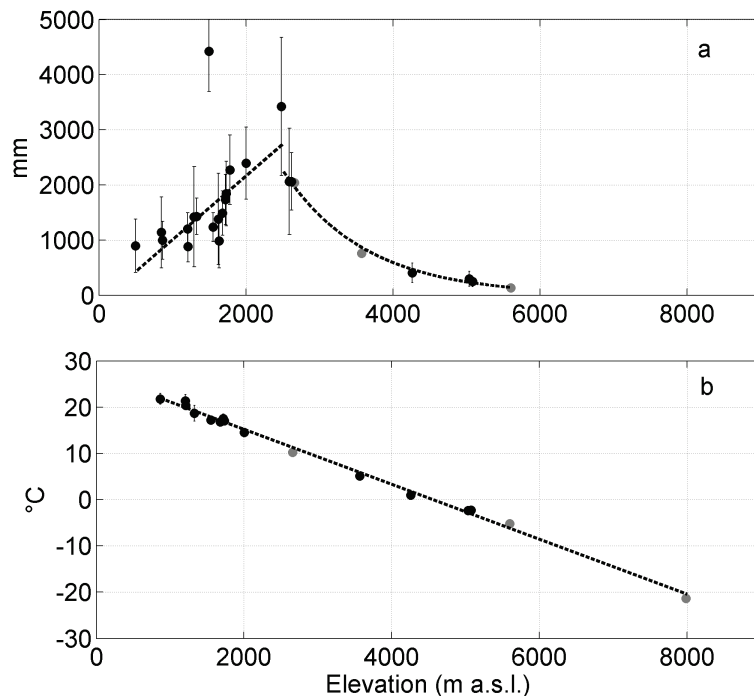


**Figure 5.** Lapse rates of **(a)** mean annual air temperature and **(b)** total annual precipitation in the Koshi Basin for the last 10 years (2003–2012). The daily missing data threshold is set to 10%. Only stations presenting at least 5 years of data (black points) are considered to create the regressions (the bars represent two SD). Gray points indicate the stations presenting less than 5 years of data.

[Title Page](#)[Abstract](#)[Introduction](#)[Conclusions](#)[References](#)[Tables](#)[Figures](#)[◀](#)[▶](#)[◀](#)[▶](#)[Back](#)[Close](#)[Full Screen / Esc](#)[Printer-friendly Version](#)[Interactive Discussion](#)

**Weak precipitation, warm winters and springs impact glaciers of Mt. Everest**

F. Salerno et al.

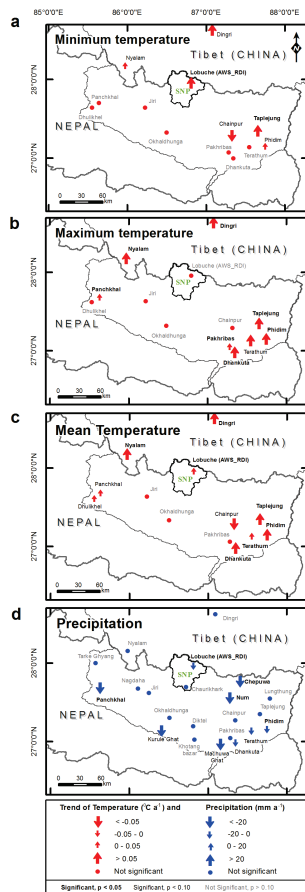


**Figure 6.** Spatial distribution of the Sen's slopes in the Koshi Basin for minimum (a), maximum (b), and mean (c) air temperature and (d) total precipitation for the 1994–2013 period. Data are reported in Table 2.

Title Page

Abstract Introduction

Conclusions References

Tables Figures

◀ ▶

◀ ▶

Back Close

Full Screen / Esc

Printer-friendly Version

Interactive Discussion

## Weak precipitation, warm winters and springs impact glaciers of Mt. Everest

F. Salerno et al.

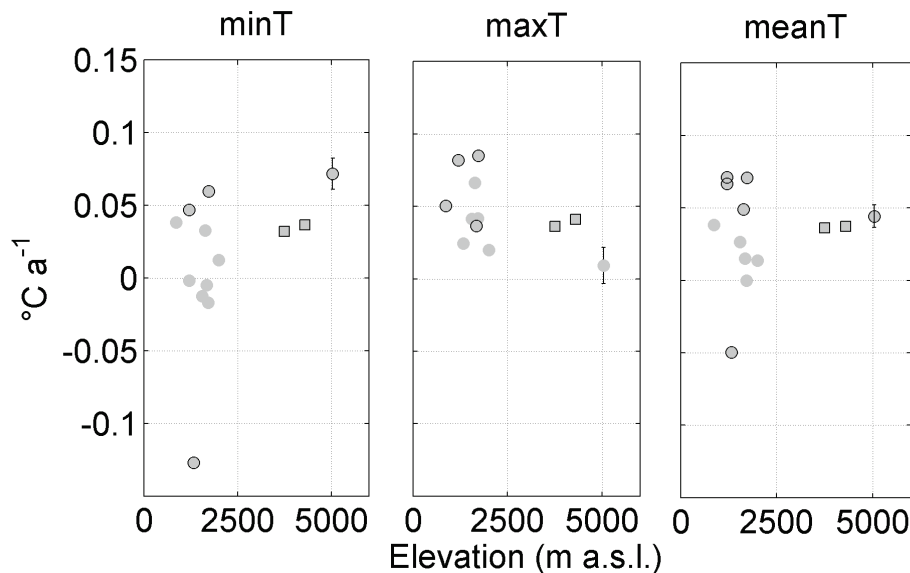


**Figure 7.** Elevation dependency of minimum (a), maximum (b), and mean (c) air temperatures with the Sen's slopes for the 1994–2013 period. The circle indicates stations with less than 10% of missing daily data, and the star indicates stations showing a trend with  $p$  value  $< 0.1$ . The red marker represents the trend and the associated uncertainty (two SD) referred to the reconstructed time series for the AWS1 station (Pyramid). Data are reported in Table 2.

Title Page

Abstract

Introduction

Conclusions

References

Tables

Figures

◀

▶

◀

▶

Back

Close

Full Screen / Esc

Printer-friendly Version

Interactive Discussion



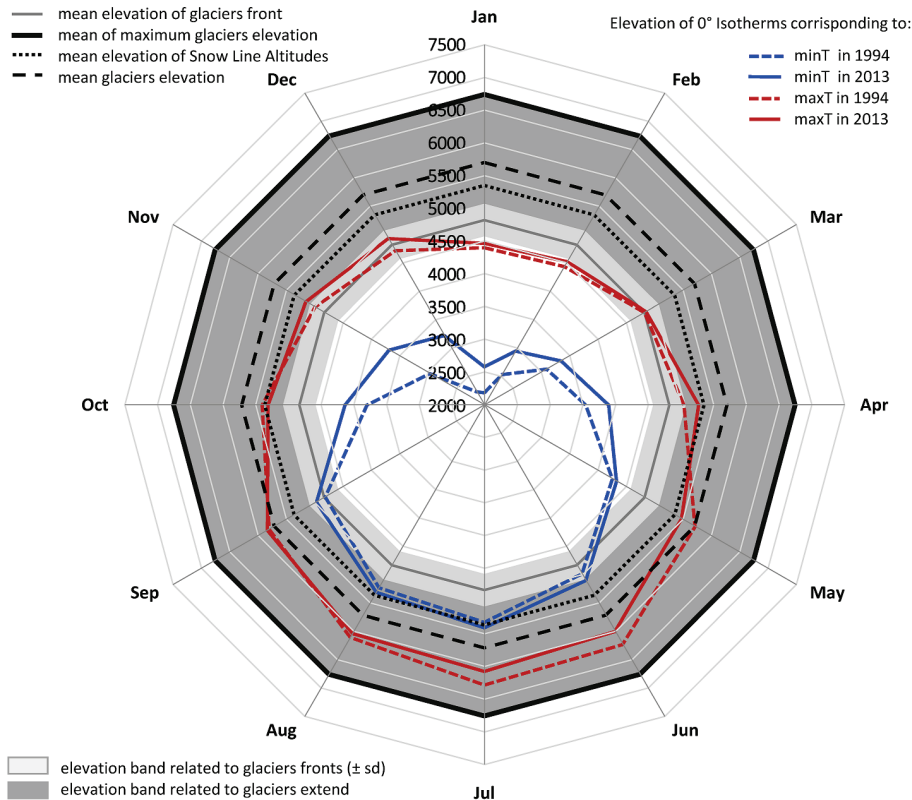


**Figure 8.** Linkage between the temperature increases and altitudinal glacier distribution. The 0°C isotherms corresponding to the mean monthly minimum and maximum temperature are plotted for the 1994 and 2013 years according the observed  $T$  trends and lapse rates.

## Weak precipitation, warm winters and springs impact glaciers of Mt. Everest

F. Salerno et al.

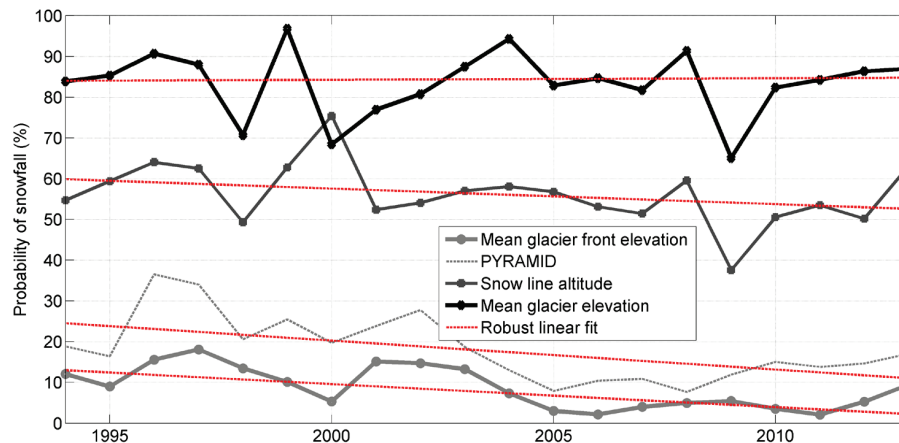


**Figure 9.** Trend analysis of annual probability of snowfall on total cumulated precipitation. The red lines represent the robust linear fitting of the time series characterized by the associated Sen's slope (more details in the caption of Fig. 3).